Biomaterials 274 (2021) 120826

Contents lists available at ScienceDirect

Biomaterials

journal homepage: www.elsevier.com/locate/biomaterials

Review

Microfluidic formulation of nanoparticles for biomedical applications

Sarah J. Shepherd [a], David Issadore [a,b,c,**,1], Michael J. Mitchell [a,d,e,f,g,*,1]

[a] Department of Bioengineering, University of Pennsylvania, Philadelphia, PA, 19104, USA
[b] Department of Electrical and Systems Engineering, University of Pennsylvania, Philadelphia, PA, 19104, USA
[c] Department of Chemical and Biomolecular Engineering, University of Pennsylvania, Philadelphia, PA, 19104, USA
[d] Abramson Cancer Center, Perelman School of Medicine, University of Pennsylvania, Philadelphia, PA, 19104, USA
[e] Institute for Immunology, Perelman School of Medicine, University of Pennsylvania, Philadelphia, PA, 19104, USA
[f] Cardiovascular Institute, Perelman School of Medicine, University of Pennsylvania, Philadelphia, PA, 19104, USA
[g] Institute for Regenerative Medicine, Perelman School of Medicine, University of Pennsylvania, Philadelphia, PA, 19104, USA

ARTICLE INFO

Keywords:
Microfluidics
Nanoparticle
Drug delivery
Imaging

ABSTRACT

Nanomedicine has made significant advances in clinical applications since the late-20th century, in part due to its distinct advantages in biocompatibility, potency, and novel therapeutic applications. Many nanoparticle (NP) therapies have been approved for clinical use, including as imaging agents or as platforms for drug delivery and gene therapy. However, there are remaining challenges that hinder translation, such as non-scalable production methods and the inefficiency of current NP formulations in delivering their cargo to their target. To address challenges with existing formulation methods that have batch-to-batch variability and produce particles with high dispersity, microfluidics—devices that manipulate fluids on a micrometer scale—have demonstrated enormous potential to generate reproducible NP formulations for therapeutic, diagnostic, and preventative applications. Microfluidic-generated NP formulations have been shown to have enhanced properties for biomedical applications by formulating NPs with more controlled physical properties than is possible with bulk techniques—such as size, size distribution, and loading efficiency. In this review, we highlight advances in microfluidic technologies for the formulation of NPs, with an emphasis on lipid-based NPs, polymeric NPs, and inorganic NPs. We provide a summary of microfluidic devices used for NP formulation with their advantages and respective challenges. Additionally, we provide our analysis for future outlooks in the field of NP formulation and microfluidics, with emerging topics of production scale-independent formulations through device parallelization and multi-step reactions within droplets.

1. Introduction

Richard Feynman famously proposed nanometer-sized materials for use in medicine in 1959, and in recent decades the field of nanomedicine has rapidly evolved for applications ranging from disease diagnosis and treatment to prevention [1–3]. Nanoparticles (NPs) are highly customizable materials that can increase solubility and stability of encapsulated cargo while decreasing toxicity by enabling controlled release and tissue specific delivery [4,5]. Additionally, NPs can deliver therapeutics—such as nucleic acids—to particular intracellular targets for potent gene therapy or can be paired with existing imaging modalities to detect disease [6,7]. A key example of the advantages of NP therapeutics is the U.S. Food and Drug Administration (FDA) approved product Doxil, a poly(ethylene glycol) (PEG)-coated liposome encapsulating the chemotherapeutic doxorubicin. Doxil achieves significantly increased circulation time and reduced side effects—such as cardiotoxicity—compared to the free drug doxorubicin [8]. Similarly, FDA approved AmBisome treats systemic infections by encapsulating amphotericin B, a drug typically insoluble in saline at pH 7, in a lipid vesicle (liposome) that reduces toxicity, increases biodistribution, and improves solubility [4]. Other FDA-approved NPs include inorganic iron NPs that have been approved for thermal ablation and iron replacement therapies (Table 1), while gold NPs are in clinical trials for photothermal therapy and gene delivery [6,9–11]. The 2018 FDA and European Medicines Agency (EMA) approval of the RNA interference NP treatment Onpattro signaled a shift in the market as more advanced therapeutic systems, such as nucleic

* Corresponding author. Department of Bioengineering, University of Pennsylvania, Philadelphia, PA, 19104, USA.
** Corresponding author. Department of Bioengineering, University of Pennsylvania, Philadelphia, PA, 19104, USA.
E-mail addresses: issadore@seas.upenn.edu (D. Issadore), mjmitch@seas.upenn.edu (M.J. Mitchell).
[1] These authors contributed equally to this work.

https://doi.org/10.1016/j.biomaterials.2021.120826
Received 20 September 2020; Received in revised form 31 March 2021; Accepted 11 April 2021
Available online 26 April 2021

acid therapies, are gaining approval [12]. Messenger RNA (mRNA) vaccines have been investigated for their high potency and potential for rapid development [13,14]—currently, two mRNA vaccines (mRNA-1273 and BNT162b2, developed by Moderna, Inc. and BioNTech/Pfizer, respectively) for the SARS-CoV-2 virus have gained emergency use authorization by the FDA and other international agencies [15–19]. As illustrated by numerous clinical applications, nanomedicine is a rapidly progressing field as it provides many opportunities for novel therapies, but still faces limitations in terms of translation from research to the clinic.

Despite advances in novel treatment options, challenges remain in the formulation, efficiency, and approval of various nanomedicines. Many NP formulations are limited by inefficient delivery to target cells and tissues, which prevents treatments from reaching the performance necessary for clinical use [25,26]. Most approved NP treatments rely on passive targeting, a process that has variable success due to: substantial patient-to-patient variation, differential stages of disease progression, and inconclusive research concerning the enhanced permeability and retention (EPR) effect in humans [9,27–29]. Active targeting approaches, including the use of ligands to direct NPs to target cell and tissue populations, have shown limited clinical efficacy as the targeting moieties can affect pharmacokinetic properties and induce opsonization [30,31]. In addition to the multitude of biological barriers for intravenous systemic delivery, NP size is a crucial parameter to control since it influences *in vivo* biodistribution, uptake, and clearance [32]. Thus, conventional formulation methods limit NP translation since they produce large or polydisperse NPs that can have batch-to-batch variability—leading to inconsistent results and processes that cannot be easily scaled from the discovery phase of a study, through animal testing, clinical testing, and finally commercial production [33–35]. Emulsion-solvent evaporation is a common bulk method for the formulation of polymeric NPs by evaporating solvent from emulsion particles, but produces particles that are large (~200 nm) that can lead to toxicity or short circulation times [36]. Bulk mixing using ultrasound, nanoprecipitation or rapid mixing methods have been applied to lipid NP and polymer NP formulations, however they are all batch processes that typically result in larger particles (>150 nm), sizes that are sub-optimal for tissue penetration and extended circulation [37–41]. Further, none of these bulk methods produce NPs in a continuous manner, leading to high degrees of batch-to-batch variation. Thus, challenges remain in consistent, reproducible formation of NPs for biomedical applications that can be translated to the clinic.

1.1. Microfluidic approaches to NP formulation

To address current challenges in NP formulation, microfluidic technologies have been used to synthesize NPs with more controlled physical properties [3]. Microfluidics enables precise control over picoliter to nanoliter volumes in devices with microscale dimensions, allowing processes such as mixing, droplet generation, or nanoprecipitation to occur with precise control not possible using conventional techniques [42]. These devices can be fabricated out of a variety of polymers, glass, silicon or paper and can be used for material generation, biosensing, tissue engineering, or microelectronic applications [43]. Soft lithography approaches, as well as advancements in device designs such as flow focusing generators, staggered herringbone micromixers, and hydrodynamic flow focusers, have accelerated nanomedicine research over the past two decades [36,44–46]. Additionally, developments in programs, such as the U.S. National Nanotechnology Coordinated Infrastructure established in 2015, have enabled users at many institutions to rapidly prototype novel designs for microfluidic devices and precisely characterize nanomaterials [47]. To demonstrate the advantages of

Table 1
Clinically approved NPs currently in use [4, 7, 9, 20–24].

Product (generic name)	Approval year	Approved designation(s)	Description
Abelcet (amphotericin B)	FDA 1995	Fungal infections	Amphotericin B lipid complex
Abraxane (paclitaxel)	FDA 2005 EMA 2008	Advanced nonsmall cell lung cancer (NSCLC) Metastatic breast cancer Metastatic pancreatic cancer	Albumin-particle bound paclitaxel
AmBisome (amphotericin B)	FDA 1997	Fungal/protozoal infections	Liposomal amphotericin B
Apealea/Paclical	EMA 2018	Ovarian cancer	Micellar formulation of paclitaxel
Curosurf (poractant alpha)	FDA 1999	Pulmonary surfactant for respiratory distress syndrome	Liposome-proteins SP-B and SP-C
InFed/CosmoFer/Ferrisat	FDA 1992 Europe 2001	Iron deficient anemia	Iron dextran colloid (low molecular weight)
DaunoXome (daunorubicin)	FDA 1996	HIV-associated Kaposi's sarcoma	Non-PEGylated liposomal daunorubicin
DepoCyt (cytarabine)	FDA 1999	Neoplastic meningitis	Liposomal cytarabine
DepoDur (morphine)	FDA 2004	Analgesia	Liposomal morphine sulfate
Diafer	Europe 2013	Iron deficiency for patients with chronic kidney disease	5% iron isomaltoside colloid
Diprivan (propofol)	FDA 1989	Anesthesia	Liposomal propofol
Doxil/Caelyx (doxorubicin)	FDA 1995 EMA 1996	Ovarian cancer HIV-associated Kaposi's sarcoma Multiple myeloma	PEGylated liposomal doxorubicin
Feraheme/Rienso (feruxmoxytol)	FDA 2009 EMA 2012	Iron replacement therapy for chronic kidney disease	Iron polyglucose sorbitol carboxymethylether colloid
Ferrlecit (ferric gluconate)	FDA 1999	Iron replacement therapy for chronic kidney disease	Iron gluconate colloid
Hensify (NBTXR3)	CE Mark 2019	Locally advanced soft cell carcinoma	Hafnium oxide NPs stimulated by radiation to induce tumor cell death
Injectafer/Ferinject (ferric carboxymaltose)	FDA 2013	Iron deficient anemia	Iron carboxymaltose colloid
Marqibo (vincristine)	FDA 2012	Acute lymphoid leukemia	Non-PEGylated liposomal vincristine
Mepact (mifarmurtide)	EMA 2009	Non-metastatic osteosarcoma	Non-PEGylated liposomal mifarmurtide
Monoferric/Monofer (ferric derisomaltose)	FDA 2020 Europe 2009	Iron deficiency anemia	10% iron isomaltoside colloid
Myocet (doxorubicin)	EMA 2000	Metastatic breast cancer	Non-PEGylated liposomal doxorubicin
NanoTherm	Europe 2010	Thermal ablation glioblastoma	Iron oxide NP
Onivyde (MM-398 irinotecan)	FDA 2015	Metastatic pancreatic cancer	PEGylated liposomal irinotecan
Onpattro (patisiran)	FDA 2018 Europe 2018	Transthyretin induced amyloidosis (hATTR)	siRNA lipid nanoparticle
Venofer (iron sucrose)	FDA 2000	Iron replacement therapy for chronic kidney disease	Iron sucrose colloid
Visudyne (verteporfin)	FDA 2000 EMA 2000	Macular degeneration	Liposomal verteporfin (light activated)
Vyxeos (daunorubicin cytarabine)	FDA 2017	Acute lymphocytic leukemia	Liposomal daunorubicin and cytarabine

microfluidics for NP synthesis, a 2008 study compared flow-focusing microfluidic and bulk synthesis of polymer NPs; they determined that microfluidics produced smaller NPs with a smaller size distribution, increased encapsulation efficiency and drug loading, as well as slower release rates [48]. Beyond enhanced control over NP properties, microfluidics offers a continuous and rapid option to produce NPs that can lead to reagent savings by enhanced loading and scalable formulation volumes [33,42,49].

Here, we review advances in microfluidic technologies for the formulation of NPs by summarizing and highlighting key examples of microfluidic designs that have had an impact on nanomedicine. We focus on applications in lipid, polymeric, and inorganic NP production to illuminate the ways in which microfluidics has allowed for control over NP size and potency, as well as optimization of formulations. Our goal throughout this article is to emphasize how microfluidics has enabled novel biomaterial discovery and provide insight into how future developments will accelerate clinical translation.

2. Liposomes and lipid nanoparticles (LNPs)

Investigation into lipid-based NPs began in the 1960s, as advances in techniques to observe lipid structures—such as electron microscopy or dynamic light scattering—enabled characterization of lipid morphology and size distribution [50–52]. As previously mentioned, many classes of drugs are either poorly soluble, unstable, or cleared from the body rapidly; thus, liposomes were evaluated to deliver small molecules or macromolecules by encapsulating them in a small aqueous compartment surrounded by a lipid bilayer [53]. Early NP applications in the 1970s focused on drug delivery using liposomes; they have since developed more advanced systems with surface coatings, such as PEG, for enhanced biodistribution and stability [54,55]. Additionally, the delivery of nucleic acids has enormous therapeutic potential ranging from

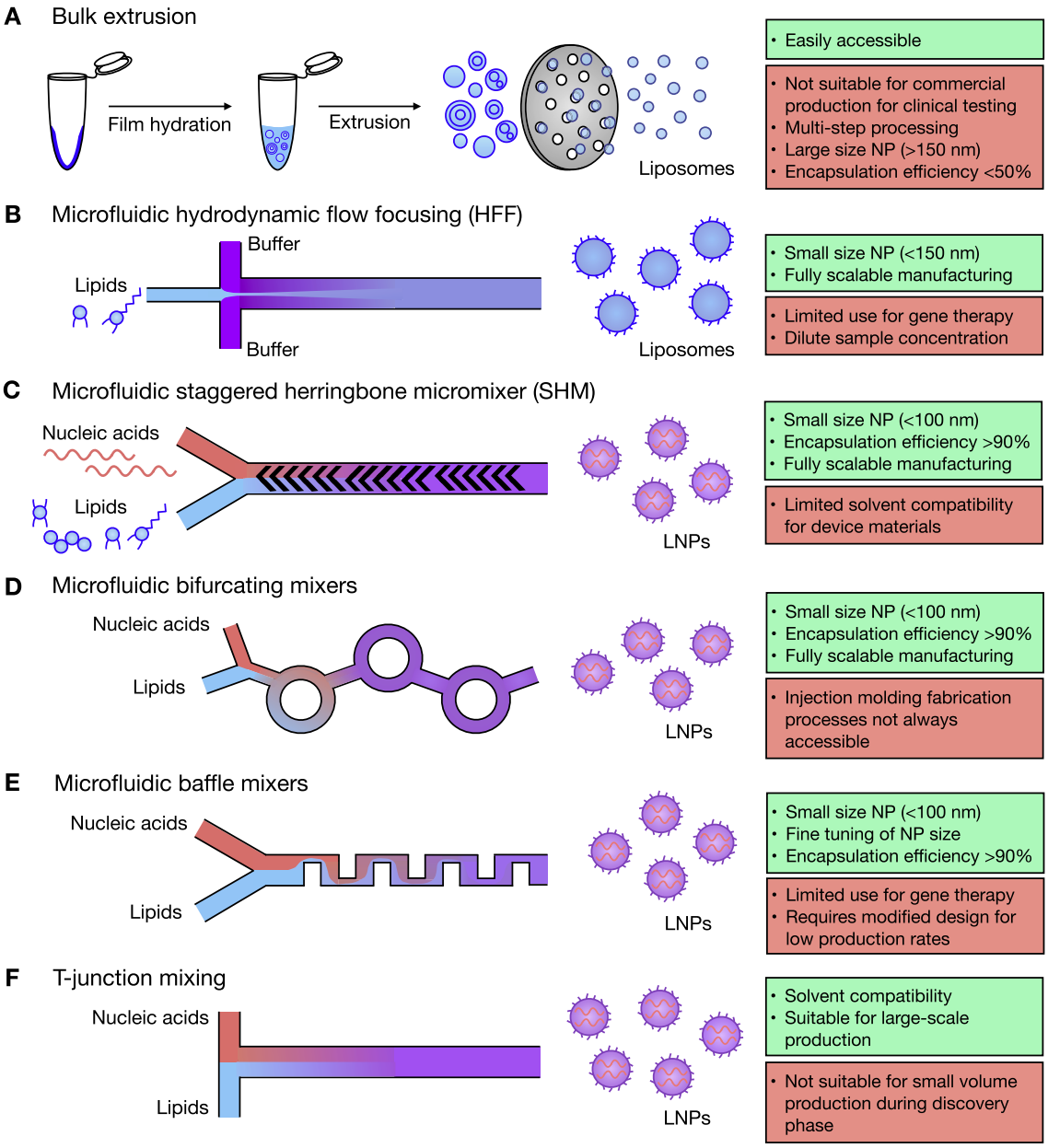

Fig. 1. Microfluidic techniques for liposome and lipid nanoparticle (LNP) formulation. Summary of bulk and microfluidic techniques for production of liposomes (A–B) and lipid nanoparticles (C–F), highlighting advantages (green) and disadvantages (red) for each. (For interpretation of the references to color in this figure legend, the reader is referred to the Web version of this article.)

immunotherapy and gene therapy to prophylactic vaccines [56–60]. However, the delivery of free nucleic acids—including small interfering RNA (siRNA) and mRNA—is limited by low transfection rates, instability, and anionic repulsions with cell membranes [7,34]. To address these challenges, synthetic delivery vehicles—such as lipid NPs (LNPs) with an electron dense core of nucleic acid/lipid complexes—have been developed due to their versatility, biocompatibility, and potent intracellular delivery of nucleic acids [61–64]. Among clinically approved NPs, liposomes and LNPs are the most advanced as they account for more than half of FDA-approved NPs that are currently in clinical use (Table 1). Here, we refer to unilamellar lipid systems with an aqueous core as liposomes, and multilamellar or electron dense lipid systems as LNPs.

2.1. Extrusion and bulk formulation

While macroscale production methods for liposomes can vary based on lipid formulations, most commercially available liposome products are manufactured by extrusion [65]. Extrusion is a multistep process where large unilamellar vesicles are formed by a process of (i) lipid film hydration, (ii) a series of freeze-thaw cycles, (iii) passing the solution through multiple filters to form liposomes (Fig. 1A), and an optional final step for (iv) encapsulation of a desired active drug [65–67]. Alternatively, liposomes can be formed in industrial scale quantities by ethanol injection, where lipids dissolved in an organic solvent are added to an aqueous suspension and extruded through multiple stacked filters to form liposomes of the desired size [66]. These processes can produce liposomes with uniform size distributions where the polydispersity index (PDI) is less than 0.1 [68], however this is variable between studies depending on the extruding pore size, number of extrusion cycles, and lipid type—with high dispersity (PDI 0.20–0.40) reported [40]. This method of membrane extrusion can be labor-intensive and subject to clogging over time due to large changes in particle size or concentrated solutions, leading to shortages of liposomal drugs, as experienced in 2011 when manufacturing issues led to a U.S. national shortage of FDA approved Doxil [40,69]. While current industrial scale production of liposomes is well-established in the field and can produce liposomes with the intended physical properties, the multi-step procedures can generate high product losses, which creates limitations when formulations involve expensive reagents [70]. Early LNP formulations for nucleic acid delivery were based on the stepwise mixing of an ethanolic lipid solution and an aqueous nucleic acid solution, where bulk mixing to precipitate LNPs was achieved by extrusion, pipette mixing, or other methods [37,71]. These methods produced LNPs with sizes greater than 100 nm—which is generally undesirable as tissue fenestrations are of a similar size, leading to a decrease in LNP tissue penetration and subsequent activity [72]. To address these manufacturing challenges and improve control over the physical properties of NPs, microfluidic approaches can be applied to liposome and LNP production.

2.2. Microfluidic hydrodynamic flow focusing (HFF)

Microfluidic strategies have been applied to LNP formulations to reduce LNP size, size dispersity and improve encapsulation efficiency. To achieve this, microfluidic devices induce nanoprecipitation of liposomes and LNPs where rapid mixing of solvent and anti-solvent promotes NP self-assembly [38]. An example of this is hydrodynamic flow focusing (HFF), a microfluidic laminar flow method in which a narrow fluid stream flows in the same channel next to a different fluid to facilitate rapid mixing between the two fluids. For example, this technique has been used to formulate liposomes by flowing an aqueous buffer on each side of a lipid-isopropyl alcohol (IPA) central stream (Fig. 1B) [73,74]. Here, the liposomes form at the buffer-IPA interface through self-assembly as they are less soluble in the buffer, and their physical properties can be controlled by changing flow rates, channel dimensions, and by the choice of lipids—with liposome sizes ranging from 30 to 200 nm [73,74]. One study found that small nucleic acid/-lipid particles (38 nm) could be formed in a HFF device and showed gene silencing *in vitro* with 20% improved encapsulation efficiency compared to bulk mixing by vortexing [75]. This microfluidic technology has also been applied to the formulation of multifunctional liposomes on chip—where the same HFF device architecture formulated three different types of liposomes: liposomes without surface modification, PEGylated liposomes, or liposomes with an active targeting ligand (folic acid) [76]. In this approach, liposomes were formulated by focusing a central stream of lipids in isopropanol with streams of PBS, where liposome size was varied from 200 nm to 55 nm based on increasing flow rate ratio of PBS to isopropanol. Another study investigated the use of a HFF device for dual-ligand liposomes, where folic acid and a cell penetrating peptide (TAT) were incorporated into a liposome that demonstrated enhanced targeting and prolonged retention in a SKOV3 xenograft tumor model compared to liposomes with a single ligand or with PEG alone [77]. Ligand density of these liposomes, an important surface property that influences cellular uptake, was found to be independent of operational flow rate ratio for both folic acid and TAT.

To further explore this technology, an advanced 3D HFF device was fabricated where the central stream of ethanol-lipid was radially focused by an aqueous buffer, where liposome size was comparable to 2D HFF devices, but throughput was increased four-fold [78]. One main disadvantage for this technique is the high flow rate ratios necessary to produce the smallest size liposomes and LNPs, leading to dilution of samples that could then require post-processing to achieve proper concentrations for *in vivo* experiments [79]. While these HFF devices have not been used as extensively as other microfluidic architectures, they provide notable advantages over conventional manufacturing techniques (extrusion, ethanol injection) as they obviate the need for post-processing and can be produced with low-cost materials [65,78].

2.3. Microfluidic staggered herringbone micromixers (SHMs)

In addition to HFF, other microfluidic strategies have been shown to improve reproducibility, increase production rates for large scale manufacturing, and improve physical properties such as encapsulation efficiency [79]. Since microfluidic systems can controllably mix solvents in microseconds to milliseconds, which is faster than the characteristic timescale for lipids to aggregate (10–100 ms), they produce smaller NPs with uniform size [42]. In 2012, two labs simultaneously demonstrated the production of LNPs for gene delivery using rapid mixing microfluidic devices that incorporate series of asymmetric protrusions called staggered herringbone micromixers (SHMs) for millisecond mixing (Fig. 1C) [37,80]. This architecture induces passive mixing by chaotic advection, where the characteristic diffusion length is greatly reduced between the ethanol-lipid and nucleic acid-buffer streams—allowing rapid, controlled mixing [44,79]. One of these studies focused on NP discovery, as the microfluidic device could mix small (10 μL) amounts of input solutions, thus saving expensive siRNA reagents and allowing more lipid structures to be screened [37]. This study found that microfluidic-produced LNPs are up to three times smaller (60–90 nm) than LNPs produced by pipette mixing (180 nm) with less size heterogeneity, which enabled the discovery of seven novel lipid structures for potent (>90%) hepatic gene silencing *in vivo* [37]. The second study showed the importance of rapid mixing rates for potent LNP production, as low flow rates produced large LNPs (170 nm) that resulted in poor gene silencing *in vivo* compared to smaller LNPs produced at high flow rates (60 nm) [80]. They determined that an increased PEG-lipid content produces progressively smaller LNPs (down to 20 nm) with a high siRNA encapsulation efficiency (>95%), while maintaining equal or superior potency to the 'gold standard' LNPs formulated with the cationic lipid DLinKC2-DMA [80]. Additionally, this study demonstrated LNP formulation at high production rates by parallelization of their device architecture, where they incorporated six SHM units into one device to produce LNPs at 72 mL/min.

These groundbreaking studies have enabled further NP discovery as more groups use microfluidic platforms for rapid, reproducible LNP production. Building on previous studies, SHM devices were used to produce siRNA LNPs of five different sizes (27 nm, 38 nm, 43 nm, 78 nm, 117 nm) with narrow size distributions by varying the PEG-lipid content [72]. Their results found that hepatic gene silencing was most efficient in LNPs ranging from 38 to 78 nm, while 27 nm LNPs were unstable, and 117 nm LNPs potentially could not pass fenestrations in liver vasculature [72]. In addition to the production of siRNA LNPs, SHM devices have been used in an investigation that varied the composition of mRNA LNPs by precisely changing the input composition of lipid structures and excipient molar ratios [81]. One study used a Design of Experiments methodology, a methodology to determine the factors that control the outcomes of a process [82], in conjunction with microfluidic formulation to rapidly identify lead formulations; their optimized formulation for mRNA delivery increased *in vivo* potency by up to 7-fold compared to previously siRNA-optimized formulations [81]. To rapidly screen more LNP formulations, molecular barcoding has been used to simultaneously measure the accumulation of many distinct LNPs in different tissues *in vivo* [25,83]. A recent study combined the high-throughput screening technique with microfluidic LNP formulation to ensure even more rapid LNP structure-activity analysis. Using SHM devices, a library of LNPs were formulated encapsulating unique DNA barcodes or Factor VII siRNA for particle accumulation or hepatic gene silencing studies, respectively—ultimately determining that this molecular barcoding platform in combination with microfluidic formulation can accelerate LNP screening to identify hit compounds [25]. In addition to LNP formulations for nucleic acid therapeutics, SHM microfluidic devices have been used for production of liposomes encapsulating hydrophobic drugs. One study encapsulated the drug propofol in a phosphatidylcholine (PC) and cholesterol liposome, identifying a 2000-fold increase of propofol solubility in a liposome (~300 mg/mL) compared to aqueous solubility (0.15 mg/mL), and a 2.5-fold increase in solubility compared to liposomes formed by sonication (~120 mg/mL) [84].

While microfluidic technologies have many advantages, one key disadvantage is the limited solvent compatibility for devices made of polydimethylsiloxane (PDMS). While these materials are common for devices fabricated by soft lithography, they can interact with organic solvents by swelling and deforming the intended structures, making them unsuitable for many formulations [85]. Additionally, channel clogging or fouling can lead to device failure due to aggregation of NP precursors on channel walls [86]. To address this challenge, some devices are made of substrates such as cyclic olefin copolymer (COC) or silicon/glass, which have excellent solvent compatibility but they require more complicated fabrication processes (i.e. injection molding or microfabrication, respectively), which can be costly and difficult to implement [87–89]. Another strategy to address challenges of clogging or fouling is surface treatment of microchannels, where devices can be "pre-fouled" by proteins or treated with polymers to control the hydrophilicity/hydrophobicity [90].

Additionally, another key disadvantage of microfluidics has been volumetric throughput. The fundamentally low production rate of microfluidic devices for the generation of materials (<10 mL/h), due to their small channels, has remained a key challenge to successfully translate the many promising laboratory-scale results of microfluidics to the larger scale production required for animal studies, clinical studies, and commercial-scale production. To address this challenge, architectures have been developed that make it possible to operate many microfluidic channels in parallel [91–93]. Ultimately, the use of SHM devices for LNP production has revolutionized nanomedicine, as it enables higher control of physical parameters and high throughput screens of NPs to enhance nucleic acid delivery.

2.4. Microfluidic bifurcating mixers and baffle mixers

The success of SHM devices has led to the commercialization of this SHM architecture for NP production by Precision NanoSystems, entitled the NanoAssemblr™ platform [79,94]. Recently, the company has introduced a novel mixing architecture called NxGen, which consists of a series of bifurcating mixers for scalable, non-turbulent mixing (Fig. 1D) [95]. These bifurcating mixers, also called toroidal mixers, induce chaotic advection as the fluid travels, the channels split into two, travel a different path length, and are then merged back together—inducing rapid mixing in a single-layer device by large centrifugal forces [96]. This bifurcating mixer architecture maintains the high encapsulation efficiency, high reproducibility, and low NP size of the original SHM design but allows production rates to be increased by 25-fold (up to 20 L/h) [95,97]. A study by Intellia Therapeutics showed *in vivo* CRISPR/Cas9 gene editing for the transthyretin gene in mice and rats following administration of co-formulated single guide RNA (sgRNA) and Cas9 mRNA LNPs. These LNPs were initially screened for gene editing *in vitro* and *in vivo* to find the optimal formulation and modification for sgRNA (formulated by the NanoAssemblr) and showed that their optimized, potent editing formulation resulted in >97% transthyretin protein knockdown for 12 months [98]. Another study optimized LNP excipients by substituting cholesterol derivatives into NPs formulated by the NanoAssemblr instrument, identifying β-sitosterol as an enhanced substitute for cholesterol in mRNA transfections *in vitro* [99]. Precision NanoSystems' instruments are highly impactful in nanomedicine, as they can be used to formulate a variety of NPs with throughput-independent formulations, in addition to the fact that they can be used by groups that are unable to perform microfluidic device fabrication [95].

In addition to bifurcating mixer devices, other microfluidic architectures have been used for controlled liposome and LNP production. One study developed a baffle mixer (Fig. 1E), or invasive LNP production device, that involves a series of perpendicular turns to rapidly mix LNP components [100]. This device produced LNPs with a mean size of 20 nm–100 nm, at intervals of 10 nm, by varying the total device flow rate, flow rate ratio, and device dimensions. Additionally, they demonstrated >90% gene silencing of Factor VII in ICR mice at a 0.1 mg/kg dose of siRNA LNPs formulated by the baffle mixer with the lipids YSK-5, cholesterol, and PEG-DMG. Overall, bifurcating mixers and baffle mixers are both single-layer devices that have shown potential for potent LNP formulations as an alternative to HFF and SHM devices.

2.5. Rapid mixing formulation

T-junction mixing, while not strictly a microfluidic process since characteristic dimensions often exceed 1 mm at turbulent (Re > 2000) conditions [101,102], is a method of rapid mixing operated at very high flow rates (40–60 mL/min) where two input streams are faced directly towards each other with a perpendicular output (Fig. 1F) [103,104]. A study by Alnylam Pharmaceuticals and Protiva Biotherapeutics found that T-junction mixing produced stable nucleic acid LNPs for potent knockdown of Apolipoprotein B (ApoB) in non-human primates following systemic administration of siRNA LNPs [105]. This study was pivotal as it was an early report of RNAi in a large animal study, showing reductions in ApoB mRNA and protein for more than 10 days [105]. A study by Merck & Co. produced siRNA LNPs targeting the murine gene *Ssb* by T-junction mixing and reduced target mRNA levels *in vivo* by over 80% [103]. Further, to reduce the acute inflammatory response following administration of LNPs, an anti-inflammatory agent (dexamethasone) was pretreated to mice and was found to mitigate cytokine responses, indicating a possible clinical strategy to achieve clinical translation [103]. Since T-junction mixing requires high flow rates, it is not always the preferred method for LNP production since it cannot be scaled down to small volumes (<100 μL) that are useful to conserve expensive reagents for high throughput screens of many different LNP formulations [37,79]. Overall, T-junction mixing offers another method for large-scale LNP production for potent gene delivery.

Macroscale processes, SHM devices, HFF devices, bifurcating mixing,

baffle mixers, and T-junction mixing can be used to produce liposomes or LNPs, each with their own advantages and disadvantages (Fig. 1). Although the aforementioned methods do not include every microfluidic approach to liposome or LNP formulation, these techniques are the most advanced, having enabled the discovery of novel NPs. These methods have greatly advanced the field of lipid-based NPs in nanomedicine, enabling treatments *in vitro*, *in vivo*, and in humans.

3. Polymeric NPs

Biodegradable polymers have been extensively researched since the 1970s for gene therapy, drug delivery, and imaging applications [106–108]. Polymeric NPs were developed for their controlled release properties that are useful for encapsulating a variety of cargo and altering release kinetics by precisely controlled variations in polymer properties [109]. For example, polycaprolactone (PCL) is a slowly degrading polymer commonly used for long-term implants where the delivery systems remain active for years, while the copolymer poly (lactic-co-glycolic) acid (PLGA) degrades at faster rates depending on ratios of its monomers, lactic acid and glycolic acid [107]. PLGA is one of the most clinically advanced polymers—with more than 15 FDA approved products that incorporate PLGA microspheres—but these applications are largely limited to local delivery and implants due to large particle size [110,111]. Polymeric NP systems have been shown to improve solubility, bioavailability, and retention time of drugs/bioactive molecules while reducing toxicity and enhancing specific tissue absorption [107,112]. Polymer drug delivery systems can be characterized by the type of release, which can be based on conventional processes (e.g. diffusion, erosion) or novel stimuli-responsive systems that undergo physical or chemical changes [113]. Advancements in polymers such as PEG have been crucial to the progress of nanomedicine; future progress in polymeric NP approaches can further improve site targeting, avoid biological barriers, and increase drug availability by improving NP physical properties [114,115].

3.1. Solvent evaporation

Solvent evaporation is a common bulk method for the formulation of polymeric NPs and microparticles, where hydrophobic or hydrophilic compounds can be encapsulated [109,116]. For hydrophobic cargo, the polymer is dissolved in an organic solvent with the intended drug, which is then added to an aqueous solution with surfactant under rapid stirring to produce an oil-in-water emulsion [109,117]. To produce polymeric NPs that encapsulate hydrophilic compounds or proteins, a water-soluble compound is added to an organic solvent with polymer to produce a water-in-oil emulsion, which is added to another aqueous solution with surfactant to produce a water-in-oil-in-water double emulsion [117]. In either case, the organic solvent is evaporated from

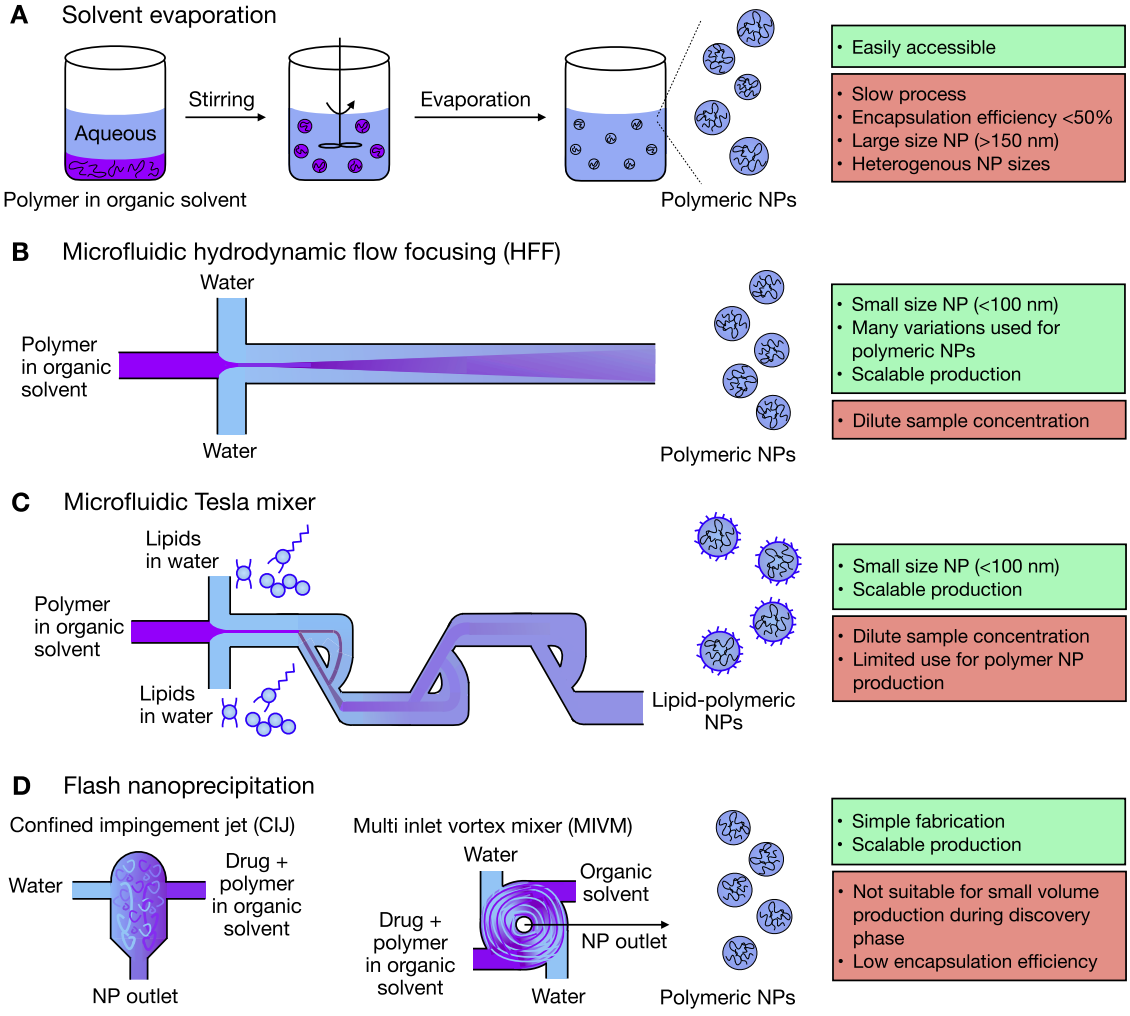

Fig. 2. Microfluidic techniques for polymeric NP synthesis. Summary of bulk and microfluidic techniques for production of polymeric NPs, highlighting advantages (green) and disadvantages (red) for each. (For interpretation of the references to color in this figure legend, the reader is referred to the Web version of this article.)

the emulsion to yield NPs (Fig. 2A) [116]. The desired parameters such as particle size and drug loading are controlled by polymer concentration, surfactant concentration, properties of each solvent, and stirring method [118]. While this production method is well-established, it has limitations as the polymeric NPs generated are large (>150 nm) with limited drug loading—leading to short biodistribution, high toxicity, and inefficient production [36]. To scale up solvent evaporation formulation of polymeric NPs, bulk stirring methods cannot precisely control emulsification, producing heterogeneous NPs that increase manufacturing costs by requiring extra processing/quality control [35, 119]. To improve production methods and precisely control NP parameters (size, polydispersity, drug loading, release kinetics), microfluidics have been applied to polymeric NP formulation.

3.2. Microfluidic HFF

3.2.1. 2D HFF

Perhaps the most studied microfluidic method to produce polymeric NPs is HFF, where a central stream of polymer in organic solvent is focused between two aqueous streams (Fig. 2B; Fig. 3A). This method of nanoprecipitation is distinct from bulk solvent evaporation as it induces self-assembly of NPs in sub-microseconds, allowing increased monodispersity, and does not require solvent evaporation [36]. One study used a HFF device to produce PLGA-PEG NPs and compared them to bulk pipette mixing—finding that microfluidic formulation maintained small particle size (34 nm) at high PLGA:PLGA-PEG content while bulk mixing produced much larger (105 nm) NPs [36]. Additionally, when encapsulating the drug docetaxel, microfluidic-formulated NPs had a longer half-life of drug release (19 h) than bulk NPs (11 h) [36]. Curcumin, a compound used to inhibit cancer cell proliferation, was encapsulated in PLGA NPs using a HFF device and showed enhanced stability (half-life 2 days) compared to free curcumin (half-life 30 min) [120]. These curcumin PLGA NPs were delivered to Jurkat and fibroblast cells *in vitro* to evaluate anticancer activity; results showed 50% maximum inhibitory response (IC_{50}) of curcumin in Jurkat cells, similar to other Jurkat studies, while not affecting fibroblast cell viability [120]. Another study comparing the encapsulation of the anticancer agent gemcitabine in PLGA NPs formulated by HFF devices and double-emulsion/solvent evaporation method—ultimately determining that entrapment efficiencies are greater by two-fold in NPs formulated by HFF, as well as a slower release of gemcitabine and more potent cytotoxicity in MCF-7 human breast adenocarcinoma cells from HFF NPs [121]. These HFF devices can also be used to produce NPs made of hyaluronic acid—a natural hydrophilic polymer—for applications in pharmaceutics or cosmetics [122]. One study showed production of hyaluronic acid NPs in a HFF device with a central aqueous phase with the polymer, focused by streams of an organic solvent, where NP sizes ranged from 140 to 460 nm depending on the flow rates and organic

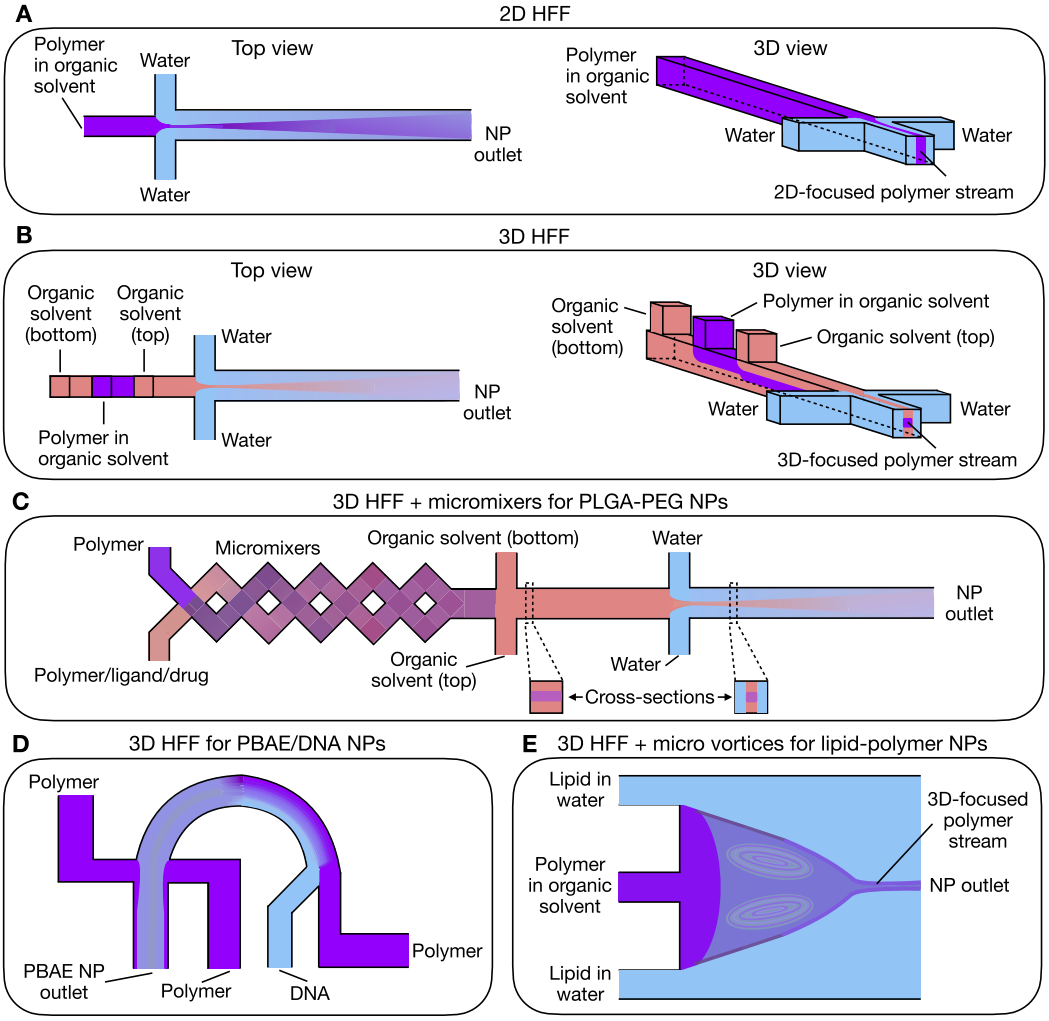

Fig. 3. Variations of hydrodynamic flow focusing (HFF) for polymeric NP production. Summary of microfluidic designs used for polymeric NP synthesis, highlighting differences between 2D HFF (A) and 3D HFF (B–E).

solvent type [122]. To increase the throughput of 2D HFF devices, one study increased the microchannel dimensions (20 μm by 50 μm to 100 μm by 200 μm) to increase production rate from 1.8 mg/h to 288 mg/h for PLGA-PEG NPs [123]. Using a similar strategy for other microfluidic architectures, maximum throughput can be increased by enlarging device features while maintaining proportionality.

3.2.2. 3D HFF

All of the previously mentioned HFF devices focus the central stream horizontally (2D HFF) to produce polymeric NPs, but not vertically in the z-direction to produce a three-dimensional focused stream (Fig. 3B). When producing polymeric NPs in 2D HFF devices, polymer aggregates can form at the central stream-device interface where channel clogs lead to device failure [124]. To avoid this, 3D HFF devices have been produced which eliminate the central stream-device interface and can produce PLGA-PEG NPs for over 10 min with no channel fouling and comparable NP properties to 2D HFF devices [124]. One study produced a parallelized 3D HFF device—with eight identical HFF channels operating at once—to show the scalability of this architecture for *in vivo* studies [125]. Using this device, Alexa-fluor 647-labelled PLGA-PEG NPs with sizes 20 nm or 35 nm were produced to evaluate pharmacokinetics and biodistribution in mice—showing similar circulation lifetime and organ accumulation for both NP sizes.

3.2.3. 3D HFF variations

There have been many variants of the 3D HFF geometry applied to the generation of polymeric NP formulations. One study screened a library of 45 PLGA-PEG NPs to evaluate the relationship between *in vitro* macrophage uptake and *in vivo* pharmacokinetics, finding that low macrophage uptake correlated with longer circulation times [126]. These NPs were produced by a modified 3D HFF device, where a micromixer upstream of flow focusing mixed NP precursors—ligands, drugs, or modified polymers (PLGA-PEG, PLGA)—prior to NP formation by nanoprecipitation in the 3D focusing region (Fig. 3C) [126]. Using this device, they formulated targeted NPs by incorporating a ligand that targets prostate-specific membrane antigen receptors overexpressed in prostate cancer cells. Their results determined a 3.5-fold increased accumulation of targeted NPs in tumors compared to non-targeted NPs [126]. Additionally, another study used an alternative design to produce poly(beta-amino ester) (PBAE) NPs for DNA delivery by focusing a DNA inlet in three dimensions by three separate polymer inlets (Fig. 3D) [127]. This device produced PBAE NPs that encapsulated GFP plasmid DNA; when delivered *in vitro* to three different cancer cell lines, the microfluidic-formulated NPs showed higher transfection and cell viability than the positive controls polyethylenimine (PEI) or Lipofectamine-2000. In addition to encapsulating multiple types of plasmid DNA for gene delivery, this study showed that microfluidic mixing produced a more homogenous product since there were fewer empty (DNA free) PBAE NPs compared to bulk mixing [127]. Another variation of the 3D HFF uses a glass capillary microfluidic device to flow an FDA-approved natural resin (shellac) and curcumin in ethanol as the inner fluid with water as the outer fluid to produce curcumin-loaded shellac NPs as natural colorants for the food industry [128]. This microfluidic strategy is a robust and reproducible method to entrap hydrophobic reagents in biocompatible NPs, where high encapsulation efficiencies are achieved (>95%) as well as reduced size and size dispersity compared to bulk production methods.

Another variant to the 3D HFF device design is the incorporation of microvortices, which can aid in the production of complex polymeric NPs. One study produced lipid-polymer NPs using a microfluidic device where microvortices form upstream of 3D flow focusing (Fig. 3E), producing NPs composed of PLGA, lecithin, and lipid-PEG that can have higher drug loading and slower release than PLGA NPs alone [129]. The microvortex-HFF device produced NPs with a lower polydispersity index (PDI ~ 0.1) and size (55–80 nm) than bulk production (PDI ~ 0.2; size 80–120 nm) at various ratios of PLGA:lipid [129]. A second study used a similar device with 3D flow focusing and microvortices to produce high-density lipoprotein (HDL)-mimicking nanomaterials for delivery of imaging and therapeutic agents [130]. The study produced HDL nanomaterials that encapsulated the hydrophobic drug simvastatin or a variety of inorganic agents—gold, iron oxide, quantum dot nanocrystals, or fluorophores—for detection by different imaging modalities such as computed tomography (CT), magnetic resonance imaging (MRI), or fluorescence microscopy [130]. This microfluidic device enabled single-step synthesis of HDL nanomaterials that maintained the same bioactive properties of native HDL, as well as maintained similar size to HDL nanomaterials produced via conventional multistep bulk processes [130]. An important physical parameter to improve is drug loading, which is generally very low (<5%) for polymeric NP systems [131]. To overcome this challenge, one study used a type of 3D HFF device—incorporating a series of three nested glass capillaries to focus the input streams in combination with turbulent mixing—to produce core/shell nanocomposites with varying compositions. These nanocomposites were formulated using a combination of PLGA, an enteric coating polymer (hypromellose acetate succinate; HF), and anticancer drugs (paclitaxel or sorafenib). Their studies demonstrated that nanocomposites with an anticancer drug core/HF shell formulated by their sequentially nested capillary microfluidic device had >42% drug loading, which is significantly greater than drug loading with a single microfluidic nanoprecipitation device (6%) or bulk precipitation (4%) [131,132]. Further efforts to improve drug loading with novel microfluidic devices will enhance NP drug delivery technologies.

A main disadvantage to HFF devices is the high flow rate ratios of the focusing streams to the central stream (20:1) needed, which can produce low concentrations of NPs that are not suitable for clinical applications without post-processing [36]. However, these devices provide many advantages for polymeric NP formulation such as high encapsulation efficiency, variety of encapsulated cargo, precise control over formulation, and scalable production [119].

3.3. Microfluidic SHM and Tesla mixer

In addition to HFF devices, other device architectures have been developed for polymeric NP formulation that overcome the over-dilution of NPs associated with HFF devices. As discussed previously in Section 2.3, SHM devices are widely used for LNP production, but can also be used for polymeric NP production. One study used an SHM device (NanoAssemblr) for the production of PLGA-PEG NPs by rapidly mixing water with an organic polymer stream; they found that the microfluidic production synthesized smaller NPs (24–43 nm) with lower polydispersity compared to NPs formed by bulk solvent evaporation synthesis (52–65 nm) [133]. Another study also used the NanoAssemblr SHM device to formulate PLGA NPs that encapsulated various proteins (ovalbumin, bovine serum albumin, or Hybrid 56) to show the optimal polymer content and flow rate to promote high protein loading [134].

Another microfluidic architecture that induces passive mixing is a Tesla mixer, which contains repeating units of channel diversions and merges for rapid mixing (Fig. 2C) [135]. This architecture has been applied to lipid-polymer NP production where a central PLGA stream is focused between lipid streams (lecithin and lipid:PEG) prior to mixing in Tesla structures [135]. By varying the lipid and polymer inputs or functionalizing the lipid inputs, the study showed NP size, charge, and stability could be varied for drug delivery applications [135]. Additionally, they formulated lipid-quantum dot NPs for imaging applications by focusing an organic quantum dot stream between lipid streams [135].

3.4. Flash nanoprecipitation

Flash nanoprecipitation—similar to T-junction mixing processes—is a millifluidic process that uses jet mixers to produce polymeric NPs. These devices are commonly called jet mixers and operate similarly at

high flow rates which induce turbulent mixing [136]. One study produced a coaxial turbulent jet mixer that was used to produce many different types of NPs (PLGA-PEG NPs, liposomes, iron oxide NPs, polystyrene (PS) NPs) that had smaller sizes with narrower size distributions compared to bulk syntheses [137]. This jet mixer was also used to produce PLGA-PEG NPs encapsulating either docetaxel or insulin for drug delivery, PS NPs encapsulating fluorescent dyes for imaging applications, and PEI NPs encapsulating siRNA for gene therapy [137]. One disadvantage for this technique is low encapsulation efficiency (10–15%) of therapeutic compounds in NPs compared to other microfluidic methods, potentially increasing production costs during large scale manufacturing [137].

In addition to jet mixers, multi inlet vortex mixers (MIVM) and confined impingement jet (CIJ) mixers rapidly mix four or two inputs, respectively (Fig. 2D) [136]. Typically, these devices are used to produce NPs made of amphiphilic block copolymers—such as PCL-*b*-PEG, PLGA-*b*-PEG, or PS-*b*-PEG—which stabilize the NP structure and encapsulate hydrophobic drugs [136,138]. One study used the MIVM to formulate PLGA NPs encapsulating SR13668—an anticancer agent with poor oral bioavailability—and showed 7-fold and 3-fold improvement in bioavailability in whole blood and plasma, respectively, over Labrasol® (a surfactant-based SR13668 formulation) following oral administration in mice [139]. Another study formulated PEG-*b*-PLGA NPs to encapsulate paclitaxel-silicate prodrugs, an anticancer agent with adjustable hydrophobicity, using a CIJ mixer [140]. By changing the silicate component of the drug, stable NPs could be formulated that showed paclitaxel-silicate NPs with faster hydrolysis rates were more effective in reducing tumor growth *in vivo* [140]. A main limitation of flash nanoprecipitation has been the high production rates that require milligrams of therapeutics during a single production batch. To address this, a micro-MIVM device was developed as a scaled-down version of the original MIVM that only requires 0.2 mg of therapeutic per production batch for rapid screening [141].

Here, we have overviewed microfluidic, millifluidic and bulk processes to produce polymeric NPs for nanomedicine. Polymeric NPs can be easily modified based on a variety of parameters (e.g. structure, type of polymer, molecular weight, or hydrophobicity); thus they are essential as drug delivery vehicles for future treatments of cancer, disease, and personalized medicine [142].

4. Inorganic NPs

Similar to organic NPs, inorganic NPs can be used as therapeutic or imaging agents due to their unique optical properties that respond to external stimuli (e.g. magnetic fields, near-infrared light) [143]. Inorganic materials such as metals, metallic oxides, and semiconductors form NPs as explained by the classical nucleation theory in steps of nucleation and growth [144]. Gold NPs are attractive as drug delivery vehicles since simple gold-thiol bioconjugation can attach targeting ligands or nucleic acids for targeted therapy [145,146]. Beyond drug delivery, gold NPs can be used as therapeutics for photothermal therapy or as contrast agents for imaging—making gold NPs one of the most highly studied NPs [147,148]. Gold NPs, along with other types of inorganic NPs such as iron colloids, are being evaluated in clinical trials (Table 1). Gold-silica nanoshells—NPs comprised of a silica core and a thin gold shell—have been investigated for targeted photothermal cancer therapy where NPs absorb near-infrared light based on the dimensions of the gold shell and can induce thermal death of tumors [149]. This nanoshell technology has been commercialized by Nanospectra Biosciences, Inc., (AuroLase Therapy) and has shown feasibility and safety in a pilot study of 16 patients for thermal ablation of prostate cancer [150]. Spherical nucleic acids, organized structures of nucleic acids conjugated to NP cores (i.e. gold NP core, liposome core), have shown potential for gene therapy and immunomodulatory applications due to their high potency and biocompatibility [151,152]. Currently, the gold core spherical nucleic acid NU-0129 (developed by Northwestern University) is being investigated in clinical trials to treat glioblastoma by delivering siRNA targeting the gene *Bcl2L12*, a gene present in glioblastoma multiforme [20,153]. Hensify (NBTXR3)—a hafnium oxide NP treatment for soft tissue sarcomas that was approved in 2019 by the European market—improves radiation therapy since the NPs have radioenhancing properties that amplify tumor cell death [20]. This platform is currently being evaluated as a standalone therapy for prostate cancer and in combination with immunotherapy to treat lung cancer [20]. As research continues to investigate inorganic NPs for therapeutic and imaging applications, advanced combinatorial treatment options could become the next-generation of nanomedicine.

Currently, inorganic NPs are synthesized by bulk formulation or microfluidic methods, such as droplet-based mixing [42]. Below, we discuss how each of these techniques is used to produce inorganic NPs, and we present advantages and disadvantages of each towards the goal of translation.

4.1. Bulk formulation

Magnetic NPs, such as iron oxide, are commonly produced by either physical or chemical methods [154]. Physical synthesis processes such as electron beam lithography or gas deposition are generally elaborate procedures which can require expensive infrastructure and produce NPs without precise control over size—a parameter that greatly impacts the catalytic and magnetic properties of the NPs themselves [154]. In chemical synthesis, iron oxide NPs are produced by coprecipitation of iron ions in high pH environments [154]. Metal NPs, including gold NPs, are commonly produced by chemical reduction where parameters such as temperature, stirring rate, and amount of reducing agent determine NP physical properties [155]. For example, one study showed that gold NP size decreased with increasing reaction temperature (from 45 nm to 15 nm) and NP size decreased with increasing ratios of reducing agent to gold salt [156]. Physical parameters such as size and surface charge also greatly impact biodistribution—gold NPs of sizes 1.8–100 nm were administered intravenously and while very small (<5 nm) gold NPs accumulated in the blood, kidneys, liver, and spleen, larger (>15 nm) gold NPs accumulated predominantly in the liver [157]. Another example of inorganic NPs are quantum dots, NPs made of semiconductor materials that have specific optical properties based on their size, where narrower size distributions correspond to sharper absorption peaks for imaging applications [42,158]. Traditional quantum dot synthesis processes are chemical methods that induce NP precipitation by combining organic solvents and semiconductor precursors with heat [158,159]. To demonstrate differences in organ accumulation due to NP size, quantum dots with a CdSe core and ZnS shell were intravenously administered to rodents, where quantum dots with size <5.5 nm were eliminated rapidly in the urine while those with larger sizes >5.5 nm accumulated in organs such as liver, lungs, spleen, and kidneys [160].

The bulk synthesis processes described above offer simple synthesis protocols, however, as these methods are scaled up for commercialization, they are faced with significant challenges. For example, these batch processes for inorganic NPs involve nucleation and growth steps occurring simultaneously (Fig. 4A) [6], resulting in a lack of control over particle growth. This leads to high levels of batch-to-batch variation in size and size distribution, which reduces the quality and reproducibility of NPs [6]. To address these challenges towards the goal of commercialization, microfluidics have been developed for inorganic NP synthesis. Below, we discuss microfluidic technologies designed to produce NPs in a continuous manner that ensures homogenous nucleation and growth [42].

4.2. Microfluidic droplet-based mixing

4.2.1. Microfluidic mixing within droplets

Droplet-based microfluidic mixing is commonly used for inorganic NP synthesis. In this technique, reactions can be confined to picoliter-

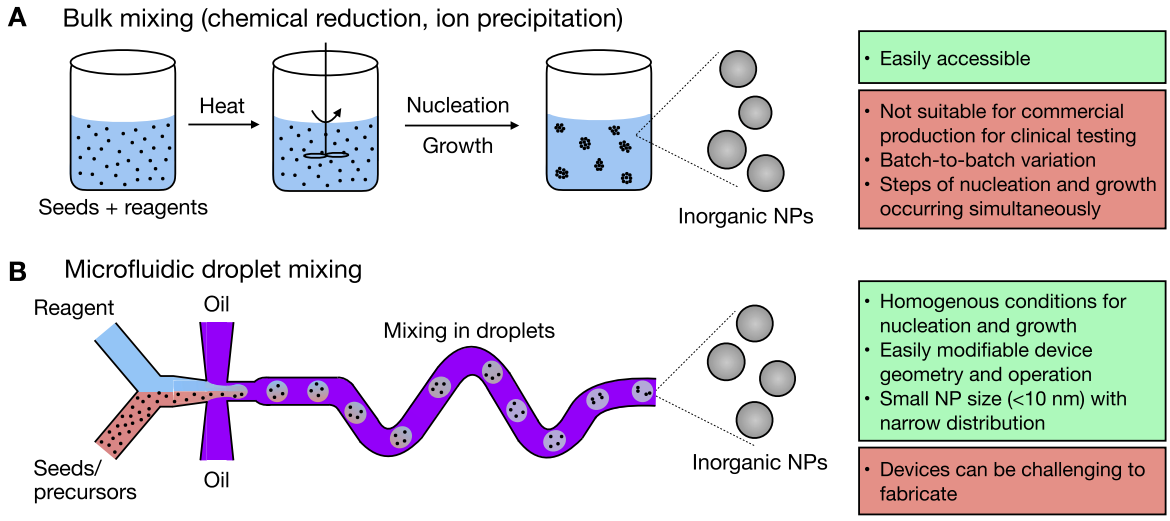

Fig. 4. Production techniques for inorganic NP synthesis. Summary of main bulk (A) and microfluidic (B) methods used to formulate inorganic NPs, highlighting advantages (green) and disadvantages (red) for each. NP, nanoparticle. (For interpretation of the references to color in this figure legend, the reader is referred to the Web version of this article.)

sized droplets, reagents do not interact with channel walls, and reaction time directly scales with channel length (Fig. 4B) [144]. Device variations can produce water-in-oil emulsions, oil-in-water emulsions, or gas bubbles for various applications [161–166] (Fig. 5). One study used a microfluidic device to produce silver NPs by combining silver nitrate with a reducing agent (tannic acid) and a stabilizing agent (trisodium citrate) in 30–80 pL size droplets, where droplet size and thus NP size were determined by input flow rates [161]. In this device, droplets are produced by a flow focusing generator and are flowed through a serpentine (or zig-zag) section that disturbs laminar flow and improves mixing efficiency (Fig. 5A) [161]. This study found that microfluidic synthesis reduced silver NP size by up to 3-fold and decreased the size distribution compared to batch synthesis, leading to a shift in the absorbance as well as a sharper absorbance peak [161]. Similarly, another study produced gold NPs or silver NPs by mixing metal salts, an ionic liquid, and a reducing agent in droplets [163]. Instead of producing droplets by a flow focusing generator, this device used a T-junction device (Fig. 5B) to form droplets that are separated by a continuous oil phase. This simple architecture allowed small (<5 nm) metal NPs to be produced in ionic liquids, which are important for NP stabilization and are compatible with common microfluidic materials such as polydimethylsiloxane (PDMS) [163]. A third study performed a

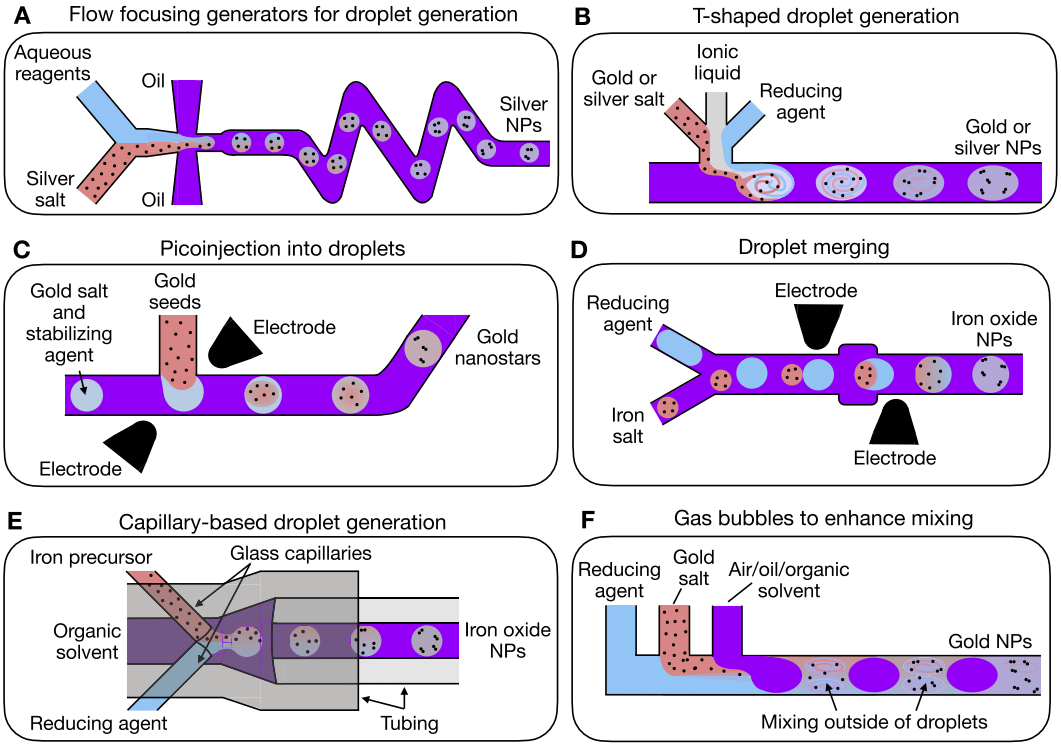

Fig. 5. Variations of droplet-based devices for inorganic NP synthesis. Summary of microfluidic designs used for inorganic NP synthesis, where mixing is performed either inside (A–E) or outside (F) of droplets.

multi-step reaction, using droplets as microreactors, to produce branched gold NPs (gold nanostars) [166]. These gold NPs have optical and spectroscopic properties that are dependent on physical parameters, which are critical properties to control for biosensing applications [166]. Initially, a gold salt and stabilizer were combined in droplets, then after a period of mixing through the channel, gold seeds were picoinjected therein (Fig. 5C). They compared these gold nanostars to those produced by another microfluidic device that used a surfactant-free method for synthesis, and found that both devices synthesized gold nanostars with reproducible branch length and density, demonstrating the precision of microfluidic devices when formulating complex NPs [166]. In addition to the aforementioned devices that bring reagents together in a co-flow system before being combined in a droplet, another droplet-based architecture was implemented to produce iron oxide NPs by merging droplets of different reagents (Fig. 5D) [165]. Using this technique, an applied electrical field merges two droplets, each containing different reagents. The two reagents, iron salts and a basic solution, form iron oxide NPs with average size 4 nm—less than half of the size of the bulk-produced NPs (mean size 9 nm) [165]. Altogether, these studies demonstrate how microfluidics offer a high level of control over NP size and dispersity. Moving forward, these microfluidic designs for mixing solutions inside of droplets should continue to be used for multi-step reactions where reaction time and reagent volumes are critical to control for the formulation of homogenous NPs.

An alternative device geometry called a capillary-based droplet reactor was used to mix iron precursors and dextran with a basic solution in droplets to form dextran-coated superparamagnetic iron oxide NPs (Fig. 5E) [162]. This device consists of two glass capillaries that intersect perpendicularly within silicone tubing, and form droplets consisting of the two reagents from each capillary that are flowed through polytetrafluoroethylene (PTFE) tubing. One main advantage of this droplet device compared to the previously discussed droplet devices is that the glass capillary system does not require lithographic patterning or surface modifications—both of which are typically required for traditional droplet-based microfluidic devices, and can complicate the fabrication process or cause device failure over time [167]. When assessed as magnetic resonance imaging (MRI) contrast agents, the iron oxide NPs displayed a high saturation magnetization and high relaxivity for a specific MRI mode, indicating their potential for contrast enhacement [162]. Additionally, these NPs had a small size (3.6 nm) with a narrow size distribution (standard deviation 0.8 nm) as well as improved stability and biocompatibility compared to bare iron oxide NPs due to the dextran coating [162].

4.2.2. Microfluidic mixing outside of droplets

Instead of mixing reagents within droplets, one study synthesized gold NPs using a microfluidic droplet device where a reducing agent and a gold precursor solution mixed outside of microdroplets by internal circulation (Fig. 5F) [164]. By changing operating parameters such as residence time and composition of droplets (air, silicone oil, or toluene), they found that gas droplets provided the best internal mixing outside of droplets and produced monodisperse small gold NPs with mean size 2.8 nm [164]. Additionally, this study introduced two different temperature zones throughout the device, where the mixing zone was maintained at room temperature using a circulating coolant fluid and the reaction zone was maintained at 100 °C. By changing the surface coating of the silicon and glass device to hydrophobic instead of hydrophilic, they formulated gold NPs by reagent mixing within droplets. Comparing these gold NPs to those formulated by reagent mixing outside of droplets, they found that mean particle size and polydispersity increased when reagents were mixed inside of droplets—mainly due to higher film thicknesses of silicone oil or toluene that reduce slip velocity and internal circulation within droplets. Overall, this study showed an interesting comparison of gold NPs formulated either within or outside of droplets, demonstrating that a single device design can be used for a variety of applications.

While microfluidic devices offer greater reproducibility and control over NP size and dispersity, their implementation is challenged by difficulties in fabrication and operation. For example, droplet merging requires precise pairing of droplets which can be impeded by small variations in flow rates or channel dimensions [165]. Further, picoinjection systems (Fig. 5C) can require the use of metal electrodes to apply the electric field, which requires additional fabrication steps to create devices [168]. As discussed earlier, glass capillary systems can provide a simpler alternative to devices that require lithographic patterning or surface coatings, but their precision and designs are more limited. As an alternative to droplet-based devices, continuous flow devices have been used for inorganic NP production—specifically for hybrid polymer-inorganic NPs.

4.3. Microfluidic HFF, SHM, T-junction mixing

Similar to LNP and polymeric NP formulations, continuous flow microfluidic devices that employ rapid mixing have been applied to inorganic NP production. One study used a 3D flow focusing device to produce an acid-degradable dextran matrix encapsulating porous silicon NPs for drug delivery [169]. An inner dispersed phase of acetalated dextran, porous silicon NPs, and therapeutics (methotrexate, paclitaxel, sorafenib) in ethanol was flowed with an outer continuous phase of polyvinyl alcohol to produce dextran-coated drug-loaded NPs by nanoprecipitation [169]. Drug release kinetics were determined by the degradation of the outer dextran polymer layer—here, they achieved a pH-responsive, 24-h release of the therapeutics methotrexate, paclitaxel, and sorafenib that was not dependent on physiochemical properties of the payload. Additionally, by conjugating an alkoxyamine-terminated poly(arginine) cell penetrating peptide to the exterior of the NPs, they improved cellular uptake and inhibited proliferation of two breast cancer cell lines compared to non-cell penetrating peptide-conjugated NPs. Microfluidic process parameters, such as flow rates, flow rate ratio, and component concentrations, were investigated to control the size (150–400 nm), PDI (~0.1), and zeta potential (−30 to −45 mV) of NPs. Additionally, this study achieved relatively high encapsulation efficiencies for the porous silicon NPs (>90%) and therapeutics (>50%) [169].

Additionally, microfluidic devices with passive mixing structures such as SHMs have been applied to encapsulate inorganic NPs within polymeric NPs for enhanced biodistribution and imaging. While larger gold NPs (>5.5 nm) can be useful since they have extended biodistribution and accumulation in diseased tissues, they present a challenge as gold NPs need to be small (<5.5 nm) to be excreted by the kidneys [170]. To address this, one study used a microfluidic SHM device to encapsulate small gold NPs into biodegradable polymeric NPs made of poly di(carboxylatophenoxy)phosphazene (PCPP) [170]. This study controlled the size of gold-PCPP NPs from 40 to 500 nm based on addition of a PEG block co-polymer and stabilized the gold cores by adding the ligands glutathione or 11-mercaptoundecanoic acid (11-MUA) [170]. Additionally, the study showed the biodegradability of gold-PCPP NPs *in vitro*, the biocompatibility of gold-PCPP NPs *in vitro* and *in vivo*, and the potential for gold-PCPP NPs to be used as potent contrast agents for computed tomography (CT) and photoacoustic (PA) imaging [170]. Notably, the gold-PCPP NP absorbance spectra shifts toward the near infrared (NIR) region compared to gold NPs alone, and produces a significantly higher PA signal at a wavelength of 700 nm for a variety of gold concentrations (1–50 μg/mL).

Spiral channels were introduced as a microfluidic method for generation of anisotropic hollow ellipsoidal mesoporous silica nanomaterials by rapid mixing of ellipsoidal mesoporous silica nanomaterials and PBS as the etching agent [171]. While synthesis of these nanomaterials in a batch reactor takes over 18 h, the microfluidic formulation is complete within seconds and tunable based on flow rates—offering a quick and reproducible production method for many types of anisotropic silica nanomaterials.

T-junction mixing has been applied to inorganic NP formulation as a continuous rapid-mixing approach to either synthesize inorganic NPs or encapsulate inorganic NPs in larger lipid-polymer NPs [102,137]. One study used a coaxial turbulent jet mixer to form sub-10 nm iron oxide NPs where an inner stream of iron oxide precursors (iron chloride in hydrochloric acid) was mixed with outer streams of tetramethylammonium hydroxide (TMAOH) [137]. Another study used a T-junction device to mix lipids and iron oxide NPs in an organic solvent with an aqueous stream to form LNPs encapsulating iron oxide NPs [102]. LNP size was varied from 36 to 154 nm depending on lipid composition and flow rate; they found that the encapsulation of iron oxide NPs did not significantly change the biodistribution as LNPs accumulated primarily in the liver [102]. When investigated for use as an MRI contrast agent, these iron oxide-LNPs provided image contrast for the spleen and liver after intravenous administration [102]. Additionally, other inorganic NPs such as gold NPs or quantum dots were encapsulated instead of iron oxide NPs to show the versatility of this approach [102].

These nanoprecipitation devices for polymeric-inorganic NP production have shown great promise for drug delivery and imaging, however, one main disadvantage to the formulation of inorganic NPs under continuous flow is channel clogging [6]. Interactions between reactants or products with channel walls can lead to accumulation and channel blockage over time, which is not a concern in droplet-based mixing [6].

5. Conclusions and future prospects

Microfluidics has been vastly applied to NP production over the past three decades—it has enhanced NP generation and discovery since they can be formulated with more controlled physical properties than comparable bulk production methods, with the potential for its production rate to be scaled up using techniques such as parallelization. Considering the importance of properties such as size, size distribution, and surface chemistry on NP activity *in vivo* [32,172,173], it is critical to use production methods that precisely control these parameters for optimal potency and minimal toxicity. A list of NPs formulated by each microfluidic device type discussed in this review is summarized in Table 2. While microfluidic NP synthesis is more advanced than microfluidic NP characterization or evaluation [42], this field is still rapidly evolving to develop novel devices and tools for nanomedicine. Remaining challenges for microfluidic NP synthesis—such as channel clogging—can lead to untimely device failure and have been thoroughly investigated in the field [174,175]. To address this problem, strategies such as 3D flow focusing have been developed for polymeric NP synthesis [124] and multiphase flows have been implemented for inorganic NP synthesis [6] to prevent interaction of NP precursors with microchannel side walls, ultimately leading to improved device performance. Future work in the field will continue to improve device architecture and operation for maximum NP efficacy.

There is growing interest in microfluidic technologies whose throughput can be scaled up beyond what is possible with single microfluidic devices, which typically produce micro-to milligram quantities of NPs (<10 mL/h) while the clinical need for NPs requires larger scales or rates of production (i.e. gram to kilogram quantities or >10 L/h) [42,176]. To achieve this, alternative designs can be used that allow for higher flow rates and pressures, or many identical channels can be patterned on the same device such that the channels run simultaneously in parallel. The latter provides a simpler solution to clinical translation, as a microfluidic design can be optimized for a single channel device, and then used for the parallelized device design. The design of a parallelized device requires high fluidic resistance to ensure uniform flow to each channel across the entire device. By incorporating microfluidic design techniques—such as small channels that increase fluidic resistance called 'flow resistors'—the design of the individual microfluidic channels is independent of the fluidic resistance of the device [92]. Using this parallelization technique, formulations can be

Table 2
Summary of different NP systems synthesized by different microfluidic devices.

Device type	Device material(s)	Type of NPs formulated	Application(s)
2D HFF	Silicon/glass; PDMS	Liposomes [73,74] Multifunctional liposomes [76] Dual-ligand liposomes [77] siRNA lipid nanoparticles [75] Docetaxel PLGA-PEG NPs [48] Curcumin PLGA NPs [120] Gemcitabine PLGA NPs [121] Hyaluronic NPs [122] PLGA-PEG NPs [123]	Drug delivery; Gene therapy; Cosmetics
3D HFF	Glass capillaries; PDMS	Liposomes [78] PLGA-PEG NPs [124,125] acid-degradable dextran matrix encapsulating porous silicon NPs [169]	Drug delivery
3D HFF variants	PDMS; Glass capillaries	PLGA or PLGA-PEG NPs [126] DNA PBAE NPs [127] Curcumin-loaded shellac NPs [128] Lipid-polymer hybrid NPs [129] HDL-mimicking nanomaterials encapsulating hydrophobic/inorganic agents [130] HF-PLGA NPs encapsulating anticancer drugs [131]	Drug delivery; Gene therapy; Natural colorant
Baffle mixer	PDMS	siRNA lipid nanoparticles [100]	Drug delivery
Droplet mixers	PDMS; Glass capillaries	Silver NPs [161,163] Gold NPs [163,164] Branched gold NPs [166] Iron oxide NPs [165] Dextran-coated superparamagnetic iron oxide NPs [162]	Imaging
Jet mixers (MIVM and CIJ)	Polycarbonate and PTFE tubing; Teflon tubing	PLGA-PEG NPs encapsulating hydrophobic drugs [137] siRNA lipid nanoparticles [137] Iron oxide NPs [137] Polystyrene NPs [137] PCL-b-PEG NPs [136,138] PLGA-b-PEG NPs [136, 138] PS-b-PEG NPs [136,138] PLGA NPs encapsulating anticancer agent [139] PEG-b-PLGA NPs encapsulating hydrophobic drugs [140]	Drug delivery; Imaging
SHM	PDMS; Cyclic olefin copolymer (COC)	siRNA lipid nanoparticles [37,72,80,81] mRNA lipid nanoparticles [81,99] DNA barcode lipid nanoparticles [25] Propofol-loaded liposomes [84] PLGA-PEG NPs [133] PLGA NPs encapsulating proteins [134] Gold PCPP NPs [170]	Drug delivery; Gene therapy; Gene editing; Imaging
Spiral channels	PDMS		Drug delivery

(*continued on next page*)

Table 2 (*continued*)

Device type	Device material(s)	Type of NPs formulated	Application(s)
T-junction mixers	Polypropylene and silicone tubing	Anisotropic hollow ellipsoidal mesoporous silica nanomaterials [171] siRNA lipid nanoparticles [103,105] Iron oxide NPs [137] Lipid nanoparticles encapsulating iron oxide NPs, gold NPs or quantum dots [102]	Drug delivery; Imaging
Tesla mixer	PDMS	Lipid-polymer NPs [135] Lipid-quantum dot NPs [135]	Drug delivery; Imaging

truly scale-independent—where the process to make micrograms or grams of the same NP are identical and result in the same physical properties.

While scale-independent technologies can address the scalability challenges associated with microfluidic NP production, challenges remain for the optimization of NP composition and structure. For drug delivery applications, the multitude of chemical structures and excipient combinations are laborious to formulate and test NPs individually [25]; thus, a microfluidic device that could formulate many unique NPs or test a variety of NPs at once could prove extremely valuable to the field. Additionally, by combining machine learning approaches [177] with rapid microfluidic formulation, more insight could be gained about the optimization of NP parameters (composition, size, zeta potential) and how each plays a role in *vitro* or *in vivo* drug delivery.

For future research, there is a clear opportunity to perform multi-step reactions in picoliter droplets, as discussed earlier with inorganic NP production [166]. This technology could perform reactions that require precise control of reaction time and reaction volumes and is not limited by the number of reaction steps or the type of NP synthesis. Droplet reactions could be applied to LNP or polymeric NP formulations that require conjugation of ligands or antibodies to the NP exterior after NPs are formulated with their intended cargo and would ensure that NPs have equal concentrations of the conjugated moiety.

Microfluidics has improved our ability to control the size, size dispersity, and encapsulation efficiency of NPs for drug delivery and imaging. With future research and new microfluidic techniques, we can continue to improve NP properties and efficacy, which will enable novel NP discovery and advance clinical translation.

Author contributions

S.J.S. performed the literature search and designed the display items. S.J.S., D.I., and M.J.M. discussed the manuscript content and wrote the manuscript. All authors critically reviewed and edited the manuscript before submission.

Declaration of competing interest

The authors declare that they have no known competing financial interests or personal relationships that could have appeared to influence the work reported in this paper.

Acknowledgements

M.J.M. acknowledges support from a Burroughs Wellcome Fund Career Award at the Scientific Interface (CASI), a US National Institutes of Health (NIH) Director's New Innovator Award (DP2 TR002776), a grant from the American Cancer Society (129784- IRG-16-188-38-IRG), the National Institutes of Health (NCI R01 CA241661, NCI R37 CA244911, and NIDDK R01 DK123049), an Abramson Cancer Center (ACC)-School of Engineering and Applied Sciences (SEAS) Discovery Grant (P30 CA016520), and a 2018 AACR- Bayer Innovation and Discovery Grant, Grant Number 18-80- 44-MITC (to M.J.M.). D.I. Acknowledges support from the Paul G. Allen Family Foundation (Reconstructing Concussion), the NIH (R33 CA206907, R21-EB023989, RM1 HG010023, R21 MH118170, R61 AI147406, the DOD (W81XWH1920002), and the Pennsylvania Department of Health (4100077083). S.J.S. is supported by an NSF Graduate Research Fellowship (Award 1845298).

References

[1] O.S. Fenton, K.N. Olafson, P.S. Pillai, M.J. Mitchell, R. Langer, Advances in biomaterials for drug delivery, Adv. Mater. 30 (29) (2018) 1–29, https://doi.org/10.1002/adma.201705328.
[2] Feynman RiP, There's plenty of room at the bottom, Eng. Sci. 23 (5) (1960).
[3] X. Zhao, F. Bian, L. Sun, L. Cai, L. Li, Y. Zhao, Microfluidic generation of nanomaterials for biomedical applications, Small 16 (9) (2020) 1–19, https://doi.org/10.1002/smll.201901943.
[4] A.C. Anselmo, S. Mitragotri, Nanoparticles in the clinic, Bioeng Transl Med 1 (1) (2016) 10–29, https://doi.org/10.1002/btm2.10003.
[5] S.E. McNeil, Nanoparticle therapeutics: a personal perspective, Wiley Interdiscip Rev Nanomedicine Nanobiotechnology 1 (3) (2009) 264–271, https://doi.org/10.1002/wnan.6.
[6] J. Ma, S.M.Y. Lee, C. Yi, C.W. Li, Controllable synthesis of functional nanoparticles by microfluidic platforms for biomedical applications-a review, Lab Chip 17 (2) (2017) 209–226, https://doi.org/10.1039/C6LC01049K.
[7] A. Akinc, M.A. Maier, M. Manoharan, et al., The Onpattro story and the clinical translation of nanomedicines containing nucleic acid-based drugs, Nat. Nanotechnol. 14 (12) (2019) 1084–1087, https://doi.org/10.1038/s41565-019-0591-y.
[8] M.E.R. O'Brien, N. Wigler, M. Inbar, et al., Reduced cardiotoxicity and comparable efficacy in a phase III trial of pegylated liposomal doxorubicin HCl (CAELYX™/Doxil®) versus conventional doxorubicin for first-line treatment of metastatic breast cancer, Ann. Oncol. 15 (3) (2004) 440–449, https://doi.org/10.1093/annonc/mdh097.
[9] D. Bobo, K.J. Robinson, J. Islam, K.J. Thurecht, S.R. Corrie, Nanoparticle-based medicines: a review of FDA-approved materials and clinical trials to date, Pharm. Res. (N. Y.) 33 (10) (2016) 2373–2387, https://doi.org/10.1007/s11095-016-1958-5.
[10] X. Huang, P.K. Jain, I.H. El-Sayed, M.A. El-Sayed, Plasmonic photothermal therapy (PPTT) using gold nanoparticles, Laser Med. Sci. 23 (3) (2008) 217–228, https://doi.org/10.1007/s10103-007-0470-x.
[11] P. Singh, S. Pandit, V.R.S.S. Mokkapati, A. Garg, V. Ravikumar, I. Mijakovic, Gold nanoparticles in diagnostics and therapeutics for human cancer, Int. J. Mol. Sci. 19 (7) (2018), https://doi.org/10.3390/ijms19071979.
[12] S.M. Hoy, Patisiran: first global approval, Drugs 78 (15) (2018) 1625–1631, https://doi.org/10.1007/s40265-018-0983-6.
[13] N. Pardi, M.J. Hogan, F.W. Porter, D. Weissman, mRNA vaccines-a new era in vaccinology, Nat. Rev. Drug Discov. 17 (4) (2018) 261–279, https://doi.org/10.1038/nrd.2017.243.
[14] A.M. Reichmuth, M.A. Oberli, A. Jaklenac, R. Langer, D. Blankschtein, mRNA vaccine delivery using lipid nanoparticles, Ther. Deliv. 7 (2016) 319–334, https://doi.org/10.4155/tde-2016-0006.
[15] L.A. Jackson, E.J. Anderson, N.G. Rouphael, et al., An mRNA vaccine against SARS-CoV-2 — preliminary report, N. Engl. J. Med. (2020), https://doi.org/10.1056/nejmoa2022483.
[16] Moderna Announces Phase 3 COVE Study of mRNA Vaccine against COVID-19 (mRNA-1273) Begins, Moderna, Inc., 2020. Published, https://investors.modernatx.com/node/9551/pdf.
[17] L. Milane, M. Amiji, Clinical approval of nanotechnology-based SARS-CoV-2 mRNA vaccines: impact on translational nanomedicine, Drug Deliv Transl Res (2021), https://doi.org/10.1007/s13346-021-00911-y, 0123456789.
[18] L.R. Baden, H.M. El Sahly, B. Essink, et al., Efficacy and safety of the mRNA-1273 SARS-CoV-2 vaccine, N. Engl. J. Med. (2020) 403–416, https://doi.org/10.1056/nejmoa2035389.
[19] F.P. Polack, S.J. Thomas, N. Kitchin, et al., Safety and efficacy of the BNT162b2 mRNA covid-19 vaccine, N. Engl. J. Med. 383 (27) (2020) 2603–2615, https://doi.org/10.1056/nejmoa2034577.
[20] A.C. Anselmo, S. Mitragotri, Nanoparticles in the clinic: an update, Bioeng Transl Med 4 (3) (2019) 1–16, https://doi.org/10.1002/btm2.10143.
[21] R. Wang, P.S. Billone, W.M. Mullett, Nanomedicine in action: an overview of cancer nanomedicine on the market and in clinical trials, J. Nanomater. 3 (6) (2013), https://doi.org/10.1155/2013/629681.
[22] A. Wicki, D. Witzigmann, V. Balasubramanian, J. Huwyler, Nanomedicine in cancer therapy: challenges, opportunities, and clinical applications, J. Contr. Release 200 (2015) 138–157, https://doi.org/10.1016/j.jconrel.2014.12.030.
[23] RNAi scores big wins, Nat. Biotechnol. 38 (1) (2020) 4, https://doi.org/10.1038/s41587-019-0384-8.
[24] S. Bisso, J.C. Leroux, Nanopharmaceuticals: a focus on their clinical translatability, Int. J. Pharm. 578 (2020), https://doi.org/10.1016/j.ijpharm.2020.119098.

[25] J.E. Dahlman, K.J. Kauffman, Y. Xing, et al., Barcoded nanoparticles for high throughput in vivo discovery of targeted therapeutics, Proc. Natl. Acad. Sci. Unit. States Am. 114 (8) (2017) 2060–2065, https://doi.org/10.1073/pnas.1620874114.

[26] M.J. Mitchell, M.M. Billingsley, R.M. Haley, M.E. Wechsler, N.A. Peppas, R. Langer, Engineering precision nanoparticles for drug delivery, Nat. Rev. Drug Discov. 20 (2) (2021) 101–124, https://doi.org/10.1038/s41573-020-0090-8.

[27] F. Danhier, To exploit the tumor microenvironment: since the EPR effect fails in the clinic, what is the future of nanomedicine? J. Contr. Release 244 (2016) 108–121, https://doi.org/10.1016/j.jconrel.2016.11.015.

[28] M.A. Miller, S. Gadde, C. Pfirschke, et al., Predicting therapeutic nanomedicine efficacy using a companion magnetic resonance imaging nanoparticle, Sci. Transl. Med. 7 (314) (2015) 1–13, https://doi.org/10.1126/scitranslmed.aac6522.

[29] M.J. Mitchell, R.K. Jain, R. Langer, Engineering and physical sciences in oncology: challenges and opportunities, Nat. Rev. Canc. 17 (11) (2017) 659–675, https://doi.org/10.1038/nrc.2017.83.

[30] G.T. Noble, J.F. Stefanick, J.D. Ashley, T. Kiziltepe, B. Bilgicer, Ligand-targeted liposome design: challenges and fundamental considerations, Trends Biotechnol. 32 (1) (2014) 32–45, https://doi.org/10.1016/j.tibtech.2013.09.007.

[31] M.R. Aronson, S.H. Medina, M.J. Mitchell, Peptide functionalized liposomes for receptor targeted cancer therapy, APL Bioeng 5 (1) (2021), https://doi.org/10.1063/5.0029860.

[32] A. Albanese, P.S. Tang, W.C.W. Chan, The effect of nanoparticle size, shape, and surface chemistry on biological systems, Annu. Rev. Biomed. Eng. 14 (1) (2012) 1–16, https://doi.org/10.1146/annurev-bioeng-071811-150124.

[33] L.H. Hung, A.P. Lee, Microfluidic devices for the synthesis of nanoparticles and biomaterials, J. Med. Biol. Eng. 27 (1) (2007) 1–6.

[34] H. Yin, R.L. Kanasty, A.A. Eltoukhy, A.J. Vegas, J.R. Dorkin, D.G. Anderson, Non-viral vectors for gene-based therapy, Nat. Rev. Genet. 15 (2014) 541–555, https://doi.org/10.1038/nrg3763.

[35] S.M. Stavis, J.A. Fagan, M. Stopa, J.A. Liddle, Nanoparticle manufacturing-heterogeneity through processes to products, ACS Appl Nano Mater 1 (9) (2018) 4358–4385, https://doi.org/10.1021/acsanm.8b01239.

[36] R. Karnik, F. Gu, P. Basto, et al., Microfluidic platform for controlled synthesis of polymeric nanoparticles, Nano Lett. 8 (9) (2008) 2906–2912, https://doi.org/10.1021/nl801736q.

[37] D. Chen, K.T. Love, Y. Chen, et al., Rapid discovery of potent siRNA-containing lipid nanoparticles enabled by controlled microfluidic formulation, J. Am. Chem. Soc. 134 (16) (2012) 6948–6951, https://doi.org/10.1021/ja301621z.

[38] Y. Liu, G. Yang, D. Zou, et al., Formulation of nanoparticles using mixing-induced nanoprecipitation for drug delivery, Ind. Eng. Chem. Res. 59 (9) (2020) 4134–4149, https://doi.org/10.1021/acs.iecr.9b04747.

[39] D.Z. Hou, C.S. Xie, K.J. Huang, C.H. Zhu, The production and characteristics of solid lipid nanoparticles (SLNs), Biomaterials 24 (10) (2003) 1781–1785, https://doi.org/10.1016/S0142-9612(02)00578-1.

[40] S.G.M. Ong, M. Chitneni, K.S. Lee, L.C. Ming, K.H. Yuen, Evaluation of extrusion technique for nanosizing liposomes, Pharmaceutics 8 (4) (2016) 1–12, https://doi.org/10.3390/pharmaceutics8040036.

[41] A.Z. Wang, R. Langer, O.C. Farokhzad, Nanoparticle delivery of cancer drugs, Annu. Rev. Med. 63 (1) (2012) 185–198, https://doi.org/10.1146/annurev-med-040210-162544.

[42] P. Valencia, O. Farokhzad, R. Karnik, R. Langer, Microfluidic technologies for accelerating the clinical translation of nanoparticles, Nat. Nanotechnol. 7 (2012) 623–629, https://doi.org/10.1038/NNANO.2012.168.

[43] G.M. Whitesides, The origins and the future of microfluidics, Nature 442 (7101) (2006) 368–373, https://doi.org/10.1038/nature05058.

[44] A.D. Stroock, S.K.W. Dertinger, A. Ajdari, I. Mezic, H.A. Stone, G.M. Whitesides, Chaotic mixer for microchannels, Science 295 (80) (2002) 647–651.

[45] Y. Xia, G.M. Whitesides, Soft lithography, Annu. Rev. Mater. Sci. 28 (1) (1998) 153–184, https://doi.org/10.1146/annurev.matsci.28.1.153.

[46] A.M. Gañán-Calvo, J.M. Gordillo, Perfectly monodisperse microbubbling by capillary flow focusing, Phys. Rev. Lett. 87 (27) (2001) 2745011–2745014, https://doi.org/10.1103/physrevlett.87.274501.

[47] About the NNCI. National Nanotechnology Coordinated Infrastructure, 2019. Published, https://www.nnci.net/about-nnci.

[48] R. Karnik, F. Gu, P. Basto, et al., Microfluidic platform for controlled synthesis of polymeric nanoparticles, Nano Lett. 8 (9) (2008) 2906–2912, https://doi.org/10.1021/nl801736q.

[49] S. Garg, G. Heuck, S. Ip, E. Ramsay, Microfluidics: a transformational tool for nanomedicine development and production, J. Drug Target. 24 (9) (2016) 821–835, https://doi.org/10.1080/1061186X.2016.1198354.

[50] A.D. Bangham, R.W. Horne, Negative staining of phospholipids and their structural modification by surface-active agents as observed in the electron microscope, J. Mol. Biol. 8 (5) (1964) 660–668, https://doi.org/10.1016/S0022-2836(64)80115-7.

[51] R. Pecora, Dynamic light scattering measurement of nanometer particles in liquids, J. Nanoparticle Res. 2 (2000) 123–131.

[52] J. Stetefeld, S.A. McKenna, T.R. Patel, Dynamic light scattering: a practical guide and applications in biomedical sciences, Biophys Rev 8 (4) (2016) 409–427, https://doi.org/10.1007/s12551-016-0218-6.

[53] L. Sercombe, T. Veerati, F. Moheimani, S.Y. Wu, A.K. Sood, S. Hua, Advances and challenges of liposome assisted drug delivery, Front. Pharmacol. 6 (DEC) (2015) 1–13, https://doi.org/10.3389/fphar.2015.00286.

[54] S. Zalipsky, Chemistry of polyethylene glycol conjugates with biologically active molecules, Adv. Drug Deliv. Rev. 16 (1995) 157–182, https://doi.org/10.1016/0169-409X(95)00023-Z.

[55] G. Gregoriadis, Liposome research in drug delivery: the early days, J. Drug Target. 16 (7–8) (2008) 520–524, https://doi.org/10.1080/10611860802228350.

[56] M.M. Billingsley, N. Singh, P. Ravikumar, R. Zhang, C.H. June, M.J. Mitchell, Ionizable lipid nanoparticle-mediated mRNA delivery for human CAR T cell engineering, Nano Lett. 20 (3) (2020) 1578–1589, https://doi.org/10.1021/acs.nanolett.9b04246.

[57] R.S. Riley, C.H. June, R. Langer, M.J. Mitchell, Delivery technologies for cancer immunotherapy, Nat. Rev. Drug Discov. 18 (3) (2019) 175–196, https://doi.org/10.1038/s41573-018-0006-z.

[58] T.K. Choueiri, M.B. Atkins, Z. Bakouny, et al., Summary from the first kidney cancer research summit, september 12-13, 2019: a focus on translational research, JNCI J Natl Cancer Inst (2020), https://doi.org/10.1093/jnci/djaa064.

[59] M.A. Oberli, A.M. Reichmuth, J.R. Dorkin, et al., Lipid nanoparticle assisted mRNA delivery for potent cancer immunotherapy, Nano Lett. 17 (3) (2017) 1326–1335, https://doi.org/10.1021/acs.nanolett.6b03329.

[60] N. Gong, N.C. Sheppard, M.M. Billingsley, C.H. June, M.J. Mitchell, Nanomaterials for T-cell cancer immunotherapy, Nat. Nanotechnol. 16 (1) (2021) 25–36, https://doi.org/10.1038/s41565-020-00822-y.

[61] A. Puri, K. Loomis, B. Smith, et al., Lipid-based nanoparticles as pharmaceutical drug carriers: from concepts to clinic, Crit. Rev. Ther. Drug Carrier Syst. 26 (6) (2009) 523–580. http://www.ncbi.nlm.nih.gov/pubmed/15619351.

[62] K.T. Love, K.P. Mahon, C.G. Levins, et al., Lipid-like materials for low-dose, in vivo gene silencing, Proc. Natl. Acad. Sci. Unit. States Am. 107 (5) (2010) 1864–1869, https://doi.org/10.1073/pnas.0910603106.

[63] A.J. Mukalel, R.S. Riley, R. Zhang, M.J. Mitchell, Nanoparticles for nucleic acid delivery: applications in cancer immunotherapy, Canc. Lett. 458 (February) (2019) 102–112, https://doi.org/10.1016/j.canlet.2019.04.040.

[64] R.S. Riley, M.V. Kashyap, M.M. Billingsley, et al., Ionizable lipid nanoparticles for in utero mRNA delivery, Sci Adv 7 (3) (2021) 1–16, https://doi.org/10.1126/sciadv.aba1028.

[65] D. Carugo, E. Bottaro, J. Owen, E. Stride, C. Nastruzzi, Liposome production by microfluidics: potential and limiting factors, Sci. Rep. 6 (2016) 1–15, https://doi.org/10.1038/srep25876.

[66] N. Maurer, K.F. Wong, H. Stark, et al., Spontaneous entrapment of polynucleotides upon electrostatic interaction with ethanol-destabilized cationic liposomes, Biophys. J. 80 (5) (2001) 2310–2326, https://doi.org/10.1016/S0006-3495(01)76202-9.

[67] S.C. Semple, A. Akinc, J. Chen, et al., Rational design of cationic lipids for siRNA delivery, Nat. Biotechnol. 28 (2) (2010) 172–176, https://doi.org/10.1038/nbt.1602.

[68] H. Jousma, H. Talsma, F. Spies, J.G.H. Joosten, H.E. Junginger, D.J. A. Crommelin, Characterization of liposomes. The influence of extrusion of multilamellar vesicles through polycarbonate membranes on particle size, particle size distribution and number of bilayers, Int. J. Pharm. 35 (3) (1987) 263–274, https://doi.org/10.1016/0378-5173(87)90139-6.

[69] J.L. Berger, A. Smith, K.K. Zorn, et al., Outcomes analysis of an alternative formulation of PEGylated liposomal doxorubicin in recurrent epithelial ovarian carcinoma during the drug shortage era, OncoTargets Ther. 7 (2014) 1409–1413, https://doi.org/10.2147/OTT.S62881.

[70] A. Wagner, K. Vorauer-Uhl, Liposome technology for industrial purposes, J Drug Deliv 2011 (2011) 1–9, https://doi.org/10.1155/2011/591325.

[71] R.L. Ball, K.A. Hajj, J. Vizelman, P. Bajaj, K.A. Whitehead, Lipid nanoparticle formulations for enhanced Co-delivery of siRNA and mRNA, Nano Lett. 18 (6) (2018) 3814–3822, https://doi.org/10.1021/acs.nanolett.8b01101.

[72] S. Chen, Y.Y.C. Tam, P.J.C. Lin, M.M.H. Sung, Y.K. Tam, P.R. Cullis, Influence of particle size on the in vivo potency of lipid nanoparticle formulations of siRNA, J. Contr. Release 235 (2016) 236–244, https://doi.org/10.1016/j.jconrel.2016.05.059.

[73] A. Jahn, W.N. Vreeland, M. Gaitan, L.E. Locascio, Controlled vesicle self-assembly in microfluidic channels with hydrodynamic focusing, J. Am. Chem. Soc. 126 (9) (2004) 2674–2675, https://doi.org/10.1021/ja0318030.

[74] A. Jahn, S.M. Stavis, J.S. Hong, W.N. Vreeland, D.L. Devoe, M. Gaitan, Microfluidic mixing and the formation of nanoscale lipid vesicles, ACS Nano 4 (4) (2010) 2077–2087, https://doi.org/10.1021/nn901676x.

[75] R. Krzysztoń, B. Salem, D.J. Lee, G. Schwake, E. Wagner, J.O. Rädler, Microfluidic self-assembly of folate-targeted monomolecular siRNA-lipid nanoparticles, Nanoscale 9 (22) (2017) 7442–7453, https://doi.org/10.1039/c7nr01593c.

[76] R. Ran, A.P.J. Middelberg, C.X. Zhao, Microfluidic synthesis of multifunctional liposomes for tumour targeting, Colloids Surf. B Biointerfaces 148 (2016) 402–410, https://doi.org/10.1016/j.colsurfb.2016.09.016.

[77] R. Ran, H. Wang, Y. Liu, et al., Microfluidic self-assembly of a combinatorial library of single- and dual-ligand liposomes for in vitro and in vivo tumor targeting, Eur. J. Pharm. Biopharm. 130 (March) (2018) 1–10, https://doi.org/10.1016/j.ejpb.2018.06.017.

[78] R.R. Hood, D.L. Devoe, J. Atencia, W.N. Vreeland, D.M. Omiatek, A facile route to the synthesis of monodisperse nanoscale liposomes using 3D microfluidic hydrodynamic focusing in a concentric capillary array, Lab Chip 14 (14) (2014) 2403–2409, https://doi.org/10.1039/c4lc00334a.

[79] M.J.W. Evers, J.A. Kulkarni, R. van der Meel, P.R. Cullis, P. Vader, R. M. Schiffelers, State-of-the-Art design and rapid-mixing production techniques of lipid nanoparticles for nucleic acid delivery, Small Methods 2 (9) (2018) 1700375, https://doi.org/10.1002/smtd.201700375.

[80] N.M. Belliveau, J. Huft, P.J. Lin, et al., Microfluidic synthesis of highly potent limit-size lipid nanoparticles for in vivo delivery of siRNA, Mol. Ther. Nucleic Acids 1 (8) (2012) e37, https://doi.org/10.1038/mtna.2012.28.

[81] K.J. Kauffman, J.R. Dorkin, J.H. Yang, et al., Optimization of lipid nanoparticle formulations for mRNA delivery in vivo with fractional factorial and definitive screening designs, Nano Lett. 15 (11) (2015) 7300–7306, https://doi.org/10.1021/acs.nanolett.5b02497.

[82] O.W. Gooding, Process optimization using combinatorial design principles: parallel synthesis and design of experiment methods, Curr. Opin. Chem. Biol. 8 (3) (2004) 297–304, https://doi.org/10.1016/j.cbpa.2004.04.009.

[83] P.P.G. Guimaraes, R. Zhang, R. Spektor, et al., Ionizable lipid nanoparticles encapsulating barcoded mRNA for accelerated in vivo delivery screening, J. Contr. Release 316 (October) (2019) 404–417, https://doi.org/10.1016/j.jconrel.2019.10.028.

[84] E. Kastner, V. Verma, D. Lowry, Y. Perrie, Microfluidic-controlled manufacture of liposomes for the solubilisation of a poorly water soluble drug, Int. J. Pharm. 485 (1–2) (2015) 122–130, https://doi.org/10.1016/j.ijpharm.2015.02.063.

[85] J. Ng Lee, C. Park, G.M. Whitesides, Solvent compatibility of poly (dimethylsiloxane)-based microfluidic devices, Anal. Chem. 75 (23) (2003) 6544–6554, https://doi.org/10.1021/ac0346712.

[86] X. Luo, P. Su, W. Zhang, C.L. Raston, Microfluidic devices in fabricating nano or micromaterials for biomedical applications, Adv Mater Technol 4 (12) (2019), https://doi.org/10.1002/admt.201900488.

[87] R. Mukhopadhyay, When PDMS isn't the best, Anal. Chem. 79 (9) (2007) 3249–3253, https://doi.org/10.1021/ac071903e.

[88] B.K. Gale, A.R. Jafek, C.J. Lambert, et al., A review of current methods in microfluidic device fabrication and future commercialization prospects, Inventions 3 (3) (2018), https://doi.org/10.3390/inventions3030060.

[89] S. Yadavali, D. Lee, D. Issadore, Robust microfabrication of highly parallelized three-dimensional microfluidics on silicon, Sci. Rep. 9 (1) (2019) 1–10, https://doi.org/10.1038/s41598-019-48515-4.

[90] R. Mukhopadhyay, When microfluidic devices go bad, Anal. Chem. 77 (21) (2005), https://doi.org/10.1021/ac053496h.

[91] T. Nisisako, T. Torii, Microfluidic large-scale integration on a chip for mass production of monodisperse droplets and particles, Lab Chip 8 (2) (2008) 287–293, https://doi.org/10.1039/b713141k.

[92] S. Yadavali, H.H. Jeong, D. Lee, D. Issadore, Silicon and glass very large scale microfluidic droplet integration for terascale generation of polymer microparticles, Nat. Commun. 9 (1) (2018), https://doi.org/10.1038/s41467-018-03515-2.

[93] H.H. Jeong, V.R. Yelleswarapu, S. Yadavali, D. Issadore, D. Lee, Kilo-scale droplet generation in three-dimensional monolithic elastomer device (3D MED), Lab Chip 15 (23) (2015) 4387–4392, https://doi.org/10.1039/c5lc01025j.

[94] C. Walsh, K. Ou, N.M. Belliveau, et al., in: K.K. Jain (Ed.), Drug Delivery System Chapter 6: Microfluidic-Based Manufacture of SiRNA-Lipid Nanoparticles for Therapeutic Applications, vol. 1141, Springer Protocols, New York, 2014, https://doi.org/10.1007/978-1-4939-0363-4_6.

[95] A. Wild, T. Leaver, R.J. Taylor, Bifurcating Mixers and Methods of Their Use and Manufacture, 2018, pp. 1–37. United States Patent No. US010076730B2, https://patentimages.storage.googleapis.com/a0/a2/5b/43416ef2d54c8f/US10076730.pdf.

[96] C. Webb, N. Forbes, C.B. Roces, et al., Using microfluidics for scalable manufacturing of nanomedicines from bench to GMP: a case study using protein-loaded liposomes, Int. J. Pharm. 582 (April) (2020) 119266, https://doi.org/10.1016/j.ijpharm.2020.119266.

[97] S. Abraham, H. Son, S.G. Talluri, et al., Robust and Scalable Manufacturing of Nucleic Acid Lipid Nanoparticles Using a Novel Micro Uidic Mixing Technology, 2020.

[98] J.D. Finn, A.R. Smith, M.C. Patel, et al., A single administration of CRISPR/Cas9 lipid nanoparticles achieves robust and persistent in vivo genome editing, Cell Rep. 22 (9) (2018) 2455–2468, https://doi.org/10.1016/j.celrep.2018.02.014.

[99] S. Patel, N. Ashwanikumar, E. Robinson, et al., Naturally-occurring cholesterol analogues in lipid nanoparticles induce polymorphic shape and enhance intracellular delivery of mRNA, Nat. Commun. 11 (1) (2020) 1–13, https://doi.org/10.1038/s41467-020-14527-2.

[100] N. Kimura, M. Maeki, Y. Sato, et al., Development of the iLiNP device: fine tuning the lipid nanoparticle size within 10 nm for drug delivery, ACS Omega 3 (5) (2018) 5044–5051, https://doi.org/10.1021/acsomega.8b00341.

[101] S. Hirota, C.T. De Ilarduya, L.G. Barron, F.C. Szoka, Simple mixing device to reproducibly prepare cationic lipid-DNA complexes (lipoplexes), Biotechniques 27 (2) (1999) 286–290, https://doi.org/10.2144/99272bm16.

[102] J.A. Kulkarni, Y.Y.C. Tam, S. Chen, et al., Rapid synthesis of lipid nanoparticles containing hydrophobic inorganic nanoparticles, Nanoscale 9 (36) (2017) 13600–13609, https://doi.org/10.1039/c7nr03272b.

[103] M.T. Abrams, M.L. Koser, J. Seitzer, et al., Evaluation of efficacy, biodistribution, and inflammation for a potent siRNA nanoparticle: effect of dexamethasone co-treatment, Mol. Ther. 18 (1) (2010) 171–180, https://doi.org/10.1038/mt.2009.208.

[104] L.B. Jeffs, L.R. Palmer, E.G. Ambegia, C. Giesbrecht, S. Ewanick, I. MacLachlan, A scalable, extrusion-free method for efficient liposomal encapsulation of plasmid DNA, Pharm. Res. (N. Y.) 22 (3) (2005) 362–372, https://doi.org/10.1007/s11095-004-1873-z.

[105] T.S. Zimmermann, A.C.H. Lee, A. Akinc, et al., RNAi-mediated gene silencing in non-human primates, Nature 441 (1) (2006) 111–114, https://doi.org/10.1038/nature04688.

[106] R. Langer, J. Folkman, Polymers for the sustained release of proteins and other macromolecules, Nature 263 (5580) (1976) 797–800, https://doi.org/10.1038/263797a0.

[107] A. Kumari, S.K. Yadav, S.C. Yadav, Biodegradable polymeric nanoparticles based drug delivery systems, Colloids Surf. B Biointerfaces 75 (1) (2010) 1–18, https://doi.org/10.1016/j.colsurfb.2009.09.001.

[108] R.M. Haley, R. Gottardi, R. Langer, M.J. Mitchell, Cyclodextrins in drug delivery: applications in gene and combination therapy, Drug Deliv Transl Res 10 (3) (2020) 661–677, https://doi.org/10.1007/s13346-020-00724-5.

[109] K.S. Soppimath, T.M. Aminabhavi, A.R. Kulkarni, W.E. Rudzinski, Biodegradable polymeric nanoparticles as drug delivery devices, J. Contr. Release 70 (2001) 1–20.

[110] P. Blasi, Poly(lactic acid)/poly(lactic-co-glycolic acid)-based microparticles: an overview, J Pharm Investig 49 (4) (2019) 337–346, https://doi.org/10.1007/s40005-019-00453-z.

[111] D.S. Kohane, Microparticles and nanoparticles for drug delivery, Biotechnol. Bioeng. 96 (2) (2007) 203–209, https://doi.org/10.1002/bit.21301.

[112] R. Zhang, M.M. Billingsley, M.J. Mitchell, Biomaterials for vaccine-based cancer immunotherapy, J. Contr. Release 292 (October) (2018) 256–276, https://doi.org/10.1016/j.jconrel.2018.10.008.

[113] W.B. Liechty, D.R. Kryscio, B.V. Slaughter, N.A. Peppas, Polymers for drug delivery systems, Annu Rev Chem Biomol Eng 1 (1) (2010) 149–173, https://doi.org/10.1146/annurev-chembioeng-073009-100847 (Polymers).

[114] A.S. Hoffman, The origins and evolution of "controlled" drug delivery systems, J. Contr. Release 132 (3) (2008) 153–163, https://doi.org/10.1016/j.jconrel.2008.08.012.

[115] J.A. Hubbell, A. Chilkoti, Nanomaterials for drug delivery, Science 337 (80) (2012) 303–305, https://doi.org/10.1126/science.1219657, 6092.

[116] P.B. O'Donnell, J.W. McGinity, Preparation of microspheres by the solvent evaporation technique, Adv. Drug Deliv. Rev. 28 (1) (1997) 25–42, https://doi.org/10.1016/S0169-409X(97)00049-5.

[117] H.K. Makadia, S. Siegel, Poly lactic-co-glycolic acid (PLGA) as biodegradable controlled drug delivery carrier, Polymers 3 (3) (2011) 1377–1397, https://doi.org/10.3390/polym3031377.

[118] P.D. Scholes, A.G.A. Coombes, L. Illum, S.S. Daviz, M. Vert, M.C. Davies, The preparation of sub-200 nm poly(lactide-co-glycolide) microspheres for site-specific drug delivery, J. Contr. Release 25 (1–2) (1993) 145–153, https://doi.org/10.1016/0168-3659(93)90103-C.

[119] E. Sah, H. Sah, Recent trends in preparation of poly(lactide-co-glycolide) nanoparticles by mixing polymeric organic solution with antisolvent, J. Nanomater. 2015 (2015), https://doi.org/10.1155/2015/794601.

[120] M.H.M. Leung, A.Q. Shen, Microfluidic assisted nanoprecipitation of PLGA nanoparticles for curcumin delivery to leukemia Jurkat cells, Langmuir 34 (13) (2018) 3961–3970, https://doi.org/10.1021/acs.langmuir.7b04335.

[121] L. Martín-Banderas, E. Sáez-Fernández, M.Á. Holgado, et al., Biocompatible gemcitabine-based nanomedicine engineered by Flow Focusing® for efficient antitumor activity, Int. J. Pharm. 443 (1–2) (2013) 103–109, https://doi.org/10.1016/j.ijpharm.2012.12.048.

[122] R.C.S. Bicudo, M.H.A. Santana, Production of hyaluronic acid (HA) nanoparticles by a continuous process inside microchannels: effects of non-solvents, organic phase flow rate, and HA concentration, Chem. Eng. Sci. 84 (2012) 134–141, https://doi.org/10.1016/j.ces.2012.08.010.

[123] T. Baby, Y. Liu, A.P.J. Middelberg, C.X. Zhao, Fundamental studies on throughput capacities of hydrodynamic flow-focusing microfluidics for producing monodisperse polymer nanoparticles, Chem. Eng. Sci. 169 (2017) 128–139, https://doi.org/10.1016/j.ces.2017.04.046.

[124] M. Rhee, P.M. Valencia, M.I. Rodriguez, R. Langer, O.C. Farokhzad, R. Karnik, Synthesis of size-tunable polymeric nanoparticles enabled by 3D hydrodynamic flow focusing in single-layer microchannels, Adv. Mater. 23 (12) (2011) 79–83, https://doi.org/10.1002/adma.201004333.

[125] J.M. Lim, N. Bertrand, P.M. Valencia, et al., Parallel microfluidic synthesis of size-tunable polymeric nanoparticles using 3D flow focusing towards in vivo study, Nanomed. Nanotechnol. Biol. Med. 10 (2) (2014) 401–409, https://doi.org/10.1016/j.nano.2013.08.003.

[126] P.M. Valencia, E.M. Pridgen, M. Rhee, R. Langer, O.C. Farokhzad, R. Karnik, Microfluidic platform for combinatorial synthesis and optimization of targeted nanoparticles for cancer therapy, ACS Nano 7 (12) (2013) 10671–10680, https://doi.org/10.1021/nn403370e.

[127] D.R. Wilson, A. Mosenia, M.P. Suprenant, et al., Continuous microfluidic assembly of biodegradable poly(Beta-amino ester)/DNA nanoparticles for enhanced gene delivery, J. Biomed. Mater. Res. 105 (6) (2017) 1813–1825, https://doi.org/10.1002/jbm.a.36033.

[128] L. Kong, R. Chen, X. Wang, et al., Controlled co-precipitation of biocompatible colorant-loaded nanoparticles by microfluidics for natural color drinks, Lab Chip 19 (12) (2019) 2089–2095, https://doi.org/10.1039/c9lc00240e.

[129] Y. Kim, B. Lee Chung, M. Ma, et al., Mass production and size control of lipid-polymer hybrid nanoparticles through controlled microvortices, Nano Lett. 12 (7) (2012) 3587–3591, https://doi.org/10.1021/nl301253v.

[130] Y. Kim, F. Fay, D.P. Cormode, et al., Single step reconstitution of multifunctional high-density lipoprotein-derived nanomaterials using microfluidics, ACS Nano 7 (11) (2013) 9975–9983, https://doi.org/10.1021/nn4039063.

[131] D. Liu, H. Zhang, S. Cito, et al., Core/shell nanocomposites produced by superfast sequential microfluidic nanoprecipitation, Nano Lett. 17 (2) (2017) 606–614, https://doi.org/10.1021/acs.nanolett.6b03251.

[132] D. Liu, S. Cito, Y. Zhang, C.F. Wang, T.M. Sikanen, H.A. Santos, A versatile and robust microfluidic platform toward high throughput synthesis of homogeneous nanoparticles with tunable properties, Adv. Mater. 27 (14) (2015) 2298–2304, https://doi.org/10.1002/adma.201405408.

[133] K. Abstiens, A.M. Goepferich, Microfluidic manufacturing improves polydispersity of multicomponent polymeric nanoparticles, J. Drug Deliv. Sci. Technol. 49 (October 2018) (2019) 433–439, https://doi.org/10.1016/j.jddst.2018.12.009.
[134] C.B. Roces, D. Christensen, Y. Perrie, Translating the fabrication of protein-loaded poly(lactic-co-glycolic acid) nanoparticles from bench to scale-independent production using microfluidics, Drug Deliv Transl Res (2020), https://doi.org/10.1007/s13346-019-00699-y.
[135] P.M. Valencia, P.A. Basto, L. Zhang, et al., Single-step assembly of homogenous lipid-polymeric and lipid-quantum dot nanoparticles enabled by microfluidic rapid mixing, ACS Nano 4 (3) (2010) 1671–1679, https://doi.org/10.1021/nn901433u.
[136] K.M. Pustulka, A.R. Wohl, H.S. Lee, et al., Flash nanoprecipitation: particle structure and stability, Mol. Pharm. 10 (11) (2013) 4367–4377, https://doi.org/10.1021/mp400337f.
[137] J.M. Lim, A. Swami, L.M. Gilson, et al., Ultra-high throughput synthesis of nanoparticles with homogeneous size distribution using a coaxial turbulent jet mixer, ACS Nano 8 (6) (2014) 6056–6065, https://doi.org/10.1021/nn501371n.
[138] W.S. Saad, R.K. Prud'Homme, Principles of nanoparticle formation by flash nanoprecipitation, Nano Today 11 (2) (2016) 212–227, https://doi.org/10.1016/j.nantod.2016.04.006.
[139] H. Shen, A.A. Banerjee, P. Mlynarska, et al., Enhanced oral bioavailability of A cancer preventive agent (SR13668) by employing polymeric nanoparticles with high drug loading, J Pharm Sci 101 (10) (2012) 3877–3885, https://doi.org/10.1002/jps.
[140] J. Han, A.R. Michel, H.S. Lee, et al., Nanoparticles containing high loads of paclitaxel-silicate prodrugs: formulation, drug release, and anticancer efficacy, Mol. Pharm. 12 (12) (2015) 4329–4335, https://doi.org/10.1021/acs.molpharmaceut.5b00530.
[141] C.E. Markwalter, R.K. Prud'homme, Design of a small-scale multi-inlet vortex mixer for scalable nanoparticle production and application to the encapsulation of biologics by inverse flash NanoPrecipitation, J Pharm Sci 107 (9) (2018) 2465–2471, https://doi.org/10.1016/j.xphs.2018.05.003.
[142] B.L. Banik, P. Fattahi, J.L. Brown, Polymeric nanoparticles: the future of nanomedicine, Wiley Interdiscip Rev Nanomedicine Nanobiotechnology 8 (2) (2016) 271–299, https://doi.org/10.1002/wnan.1364.
[143] A.C. Anselmo, S. Mitragotri, A review of clinical translation of inorganic nanoparticles, AAPS J. 17 (5) (2015) 1041–1054, https://doi.org/10.1208/s12248-015-9780-2.
[144] A. Abou-Hassan, O. Sandre, V. Cabuil, Microfluidics for inorganic chemistry, Angew. Chem. Int. Ed. 49 (36) (2010) 6268–6286, https://doi.org/10.1002/anie.200904285.
[145] H. Daraee, A. Eatemadi, E. Abbasi, S.F. Aval, M. Kouhi, A. Akbarzadeh, Application of gold nanoparticles in biomedical and drug delivery. *Artif Cells*, Nanomedicine Biotechnol 44 (1) (2016) 410–422, https://doi.org/10.3109/21691401.2014.955107.
[146] P.P.G. Guimarães, S. Gaglione, T. Sewastianik, R.D. Carrasco, R. Langer, M. J. Mitchell, Nanoparticles for immune cytokine TRAIL-based cancer therapy, ACS Nano 12 (2) (2018) 912–931, https://doi.org/10.1021/acsnano.7b05876.
[147] Y. Ding, Z. Jiang, K. Saha, et al., Gold nanoparticles for nucleic acid delivery, Mol. Ther. 22 (6) (2014) 1075–1083, https://doi.org/10.1038/mt.2014.30.
[148] S. Jain, D.G. Hirst, J.M. O'Sullivan, Gold nanoparticles as novel agents for cancer therapy, Br. J. Radiol. 85 (1010) (2012) 101–113, https://doi.org/10.1259/bjr/59448833.
[149] Y. Liu, B.M. Crawford, T. Vo-Dinh, Gold nanoparticles-mediated photothermal therapy and immunotherapy, Immunotherapy 10 (13) (2018) 1175–1188, https://doi.org/10.2217/imt-2018-0029.
[150] A.R. Rastinehad, H. Anastos, E. Wajswol, et al., Gold nanoshell-localized photothermal ablation of prostate tumors in a clinical pilot device study, Proc. Natl. Acad. Sci. U. S. A. 116 (37) (2019) 18590–18596, https://doi.org/10.1073/pnas.1906929116.
[151] A.F. Radovic-Moreno, N. Chernyak, C.C. Mader, et al., Immunomodulatory spherical nucleic acids, Proc. Natl. Acad. Sci. U. S. A. 112 (13) (2015) 3892–3897, https://doi.org/10.1073/pnas.1502850112.
[152] D. Zheng, D.A. Giljohann, D.L. Chen, et al., Topical delivery of siRNA-based spherical nucleic acid nanoparticle conjugates for gene regulation, Proc. Natl. Acad. Sci. U. S. A. 109 (30) (2012) 11975–11980, https://doi.org/10.1073/pnas.1118425109.
[153] C.H. Kapadia, J.R. Melamed, E.S. Day, Spherical nucleic acid nanoparticles: therapeutic potential, BioDrugs 32 (4) (2018) 297–309, https://doi.org/10.1007/s40259-018-0290-5.
[154] A. Ali, H. Zafar, M. Zia, et al., Synthesis, characterization, applications, and challenges of iron oxide nanoparticles, Nanotechnol. Sci. Appl. 9 (2016) 49–67, https://doi.org/10.2147/NSA.S99986.
[155] C. Daruich De Souza, B. Ribeiro Nogueira, M.E.C.M. Rostelato, Review of the methodologies used in the synthesis gold nanoparticles by chemical reduction, J. Alloys Compd. 798 (2019) 714–740, https://doi.org/10.1016/j.jallcom.2019.05.153.
[156] J. Dong, P.L. Carpinone, G. Pyrgiotakis, P. Demokritou, B.M. Moudgil, Synthesis of precision gold nanoparticles using Turkevich method, KONA Powder Part J 37 (August) (2020) 224–232, https://doi.org/10.14356/kona.2020011.
[157] S. Hirn, M. Semmler-Behnke, C. Schleh, et al., Particle size-dependent and surface charge-dependent biodistribution of gold nanoparticles after intravenous administration, Eur. J. Pharm. Biopharm. 77 (3) (2011) 407–416, https://doi.org/10.1016/j.ejpb.2010.12.029.
[158] A. Valizadeh, H. Mikaeili, M. Samiei, et al., Quantum dots: synthesis, bioapplications, and toxicity, Nanoscale Res Lett 7 (1) (2012) 1, https://doi.org/10.1186/1556-276X-7-480.
[159] Y. Pu, F. Cai, D. Wang, J.X. Wang, J.F. Chen, Colloidal synthesis of semiconductor quantum dots toward large-scale production: a review, Ind. Eng. Chem. Res. 57 (6) (2018) 1790–1802, https://doi.org/10.1021/acs.iecr.7b04836.
[160] H.S. Choi, W. Liu, P. Misra, et al., Renal clearance of nanoparticles, Nat. Biotechnol. 25 (10) (2007) 1165–1170, https://doi.org/10.1038/nbt1340.Renal.
[161] O. Kašpar, A.H. Koyuncu, A. Pittermannová, P. Ulbrich, V. Tokárová, Governing factors for preparation of silver nanoparticles using droplet-based microfluidic device, Biomed. Microdevices 21 (4) (2019) 1–14, https://doi.org/10.1007/s10544-019-0435-4.
[162] K. Kumar, A.M. Nightingale, S.H. Krishnadasan, et al., Direct synthesis of dextran-coated superparamagnetic iron oxide nanoparticles in a capillary-based droplet reactor, J. Mater. Chem. 22 (11) (2012) 4704–4708, https://doi.org/10.1039/c2jm30257h.
[163] L.L. Lazarus, C.T. Riche, B.C. Marin, M. Gupta, N. Malmstadt, R.L. Brutchey, Two-phase microfluidic droplet flows of ionic liquids for the synthesis of gold and silver nanoparticles, ACS Appl. Mater. Interfaces 4 (6) (2012) 3077–3083, https://doi.org/10.1021/am3004413.
[164] V. Sebastian Cabeza, S. Kuhn, A.A. Kulkarni, K.F. Jensen, Size-controlled flow synthesis of gold nanoparticles using a segmented flow microfluidic platform, Langmuir 28 (17) (2012) 7007–7013, https://doi.org/10.1021/la205131e.
[165] L. Frenz, A. El Harrak, M. Pauly, S. Bégin-Colin, A.D. Griffiths, J.C. Baret, Droplet-based microreactors for the synthesis of magnetic iron oxide nanoparticles, Angew. Chem. Int. Ed. 47 (36) (2008) 6817–6820, https://doi.org/10.1002/anie.200801360.
[166] S. Abalde-Cela, P. Taladriz-Blanco, M.G. De Oliveira, C. Abell, Droplet microfluidics for the highly controlled synthesis of branched gold nanoparticles, Sci. Rep. 8 (1) (2018) 1–6, https://doi.org/10.1038/s41598-018-20754-x.
[167] A.M. Nightingale, S.H. Krishnadasan, D. Berhanu, et al., A stable droplet reactor for high temperature nanocrystal synthesis, Lab Chip 11 (7) (2011) 1221–1227, https://doi.org/10.1039/c0lc00507j.
[168] B. O'Donovan, D.J. Eastburn, A.R. Abate, Electrode-free picoinjection of microfluidic drops, Lab Chip 12 (20) (2012) 4029–4032, https://doi.org/10.1039/c2lc40693d.
[169] D. Liu, H. Zhang, E. Mäkilä, et al., Microfluidic assisted one-step fabrication of porous silicon@acetalated dextran nanocomposites for precisely controlled combination chemotherapy, Biomaterials 39 (2015) 249–259, https://doi.org/10.1016/j.biomaterials.2014.10.079.
[170] R. Cheheltani, R.M. Ezzibdeh, P. Chhour, et al., Tunable, biodegradable gold nanoparticles as contrast agents for computed tomography and photoacoustic imaging, Biomaterials 102 (2016) 87–97, https://doi.org/10.1016/j.biomaterials.2016.06.015.
[171] N. Hao, Y. Nie, A. Tadimety, A.B. Closson, J.X.J. Zhang, Microfluidics-mediated self-template synthesis of anisotropic hollow ellipsoidal mesoporous silica nanomaterials, Mater Res Lett 5 (8) (2017) 584–590, https://doi.org/10.1080/21663831.2017.1376720.
[172] E.A. Sykes, J. Chen, G. Zheng, W.C.W. Chan, Investigating the impact of nanoparticle size on active and passive tumor targeting efficiency, ACS Nano 8 (6) (2014) 5696–5706, https://doi.org/10.1021/nn500299p.
[173] N. Hoshyar, S. Gray, H. Han, G. Bao, The effect of nanoparticle size on in vivo pharmacokinetics and cellular interaction, Nanomedicine 11 (6) (2016) 673–692.
[174] E. Dressaire, A. Sauret, Clogging of microfluidic systems, Soft Matter 13 (1) (2017) 37–48, https://doi.org/10.1039/C6SM01879C.
[175] H.M. Wyss, D.L. Blair, J.F. Morris, H.A. Stone, D.A. Weitz, Mechanism for clogging of microchannels, Phys. Rev. E - Stat. Nonlinear Soft Matter Phys. 74 (6) (2006) 1–4, https://doi.org/10.1103/PhysRevE.74.061402.
[176] L. Zhang, Q. Chen, Y. Ma, J. Sun, Microfluidic methods for fabrication and engineering of nanoparticle drug delivery systems, ACS Appl Bio Mater 3 (1) (2020) 107–120, https://doi.org/10.1021/acsabm.9b00853.
[177] G. Yamankurt, E.J. Berns, A. Xue, et al., Exploration of the nanomedicine-design space with high-throughput screening and machine learning, Nat Biomed Eng 3 (4) (2019) 318–327, https://doi.org/10.1038/s41551-019-0351-1.